DOI: 10.1002/chem.201102692

Mechanism of the Transition-Metal-Catalyzed Hydroarylation of Bromo-Alkynes Revisited: Hydrogen versus Bromine Migration

Genping Huang,[a, c] Bing Cheng,[a] Liang Xu,[a] Yahong Li,*[b] and Yuanzhi Xia*[a]

Abstract: A comprehensive mechanistic study of the $InCl_3$-, AuCl-, and $PtCl_2$-catalyzed cycloisomerization of the 2-(haloethynyl)biphenyl derivatives of Fürstner et al. was carried out by DFT/M06 calculations to uncover the catalyst-dependent selectivity of the reactions. The results revealed that the 6-*endo*-dig cyclization is the most favorable pathway in both $InCl_3$- and AuCl-catalyzed reactions. When AuCl is used, the 9-bromophenanthrene product could be formed by consecutive 1,2-H/1,2-Br migrations from the Wheland-type intermediate of the 6-*endo*-dig cyclization. However, in the $InCl_3$-catalyzed reactions, the chloride-assisted intermolecular H-migrations between two Wheland-type intermediates are more favorable. These Cl-assisted H-migrations would eventually lead to 10-bromophenanthrene through protodemetalation of the aryl indium intermediate with HCl. The cause of the poor selectivity of the $PtCl_2$ catalyst in the experiments by the Fürstner group was predicted. It was found that both the $PtCl_2$-catalyzed alkyne–vinylidene rearrangement and the 5-*exo*-dig cyclization pathways have very close activation energies. Further calculations found the former pathway would lead eventually to both 9- and 10-bromophenanthrene products, as a result of the Cl-assisted H-migrations after the cyclization of the Pt–vinylidene intermediate. Alternatively, the intermediate from the 5-*exo*-dig cyclization would be transformed into a relatively stable Pt–carbene intermediate irreversibly, which could give rise to the 9-alkylidene fluorene product through a 1,2-H shift with a 28.1 kcal mol^{-1} activation barrier. These findings shed new light on the complex product mixtures of the $PtCl_2$-catalyzed reaction.

Keywords: alkynes · cycloisomerization · density functional calculations · hydroarylation · transition metals

Introduction

Interest in the cycloisomerizations of alkenes, alkynes, and allenes catalyzed by gold,[1] platinum,[2] and other soft Lewis acids[3] has undergone a marked increase in the past decade. In most of these reactions, the cycloisomerization is initiated with the electrophilic activation of the unsaturated moiety by a carbophilic metal catalyst, followed by the intramolecular attack of a nucleophile.[1d,4,5] Previous studies have shown that the gold-catalyzed reactions are sensitive to subtle structural and electronic changes of the substrate,[6] and many of them are influenced dramatically by the ligand,[7] solvent,[8] and additive.[9] Thus, peculiar catalytic activity of gold complexes is often observed relative to other Lewis acid catalysts.[10,11]

The intramolecular hydroarylation of unsaturated precursors gives rise to fused aromatic compounds in an atom-economic fashion.[12] A seminal study from the Fürstner group[13] disclosed that the alkynylated and allenylated biaryl derivatives undergo cycloisomerization readily under the catalysis of $PtCl_2$, AuCl, $GaCl_3$,[3b,14] and $InCl_3$,[15,16] providing a flexible approach to phenanthrenes and polycyclic heteroarenes. Interesting regiochemistry was observed for different catalysts and precursors.[13] As shown in Scheme 1, regiodivergent synthesis of 9-halo- and 10-halophenanthrenes (**B** and **C**, respectively) from halo-alkyne **A** could be realized by switching the catalyst from AuCl to $InCl_3$.[17] However, the use of $PtCl_2$ as the catalyst would result in complex product mixtures.[13a,b] According to the originally proposed mechanism by the Fürstner group,[13] the formation of a rare vinylidene intermediate (intermediate ***i*** in Scheme 2) may account for the gold-catalyzed 1,2-halide migration.[18,19] Alternatively, the formation of 10-halophenanthrene under $InCl_3$ catalysis is believed to originate from the 6-*endo*-dig cyclization of reactant **A** (formation of intermediate ***ii*** in Scheme 2).[13]

[a] Dr. G. Huang, B. Cheng, L. Xu, Prof. Dr. Y. Xia
College of Chemistry and Materials Engineering
Wenzhou University
Wenzhou 325035 (P. R. China)
Fax: (+86) 86689300
E-mail: xyz@wzu.edu.cn

[b] Prof. Dr. Y. Li
College of Chemistry, Chemical Engineering, and Materials Science
Soochow University
Suzhou 215123 (P. R. China)
E-mail: liyahong@suda.edu.cn

[c] Dr. G. Huang
Qinghai Institute of Salt Lakes
Chinese Academy of Sciences
Xining 810008 (P. R. China)

Supporting information for this article is available on the WWW under http://dx.doi.org/10.1002/chem.201102692.

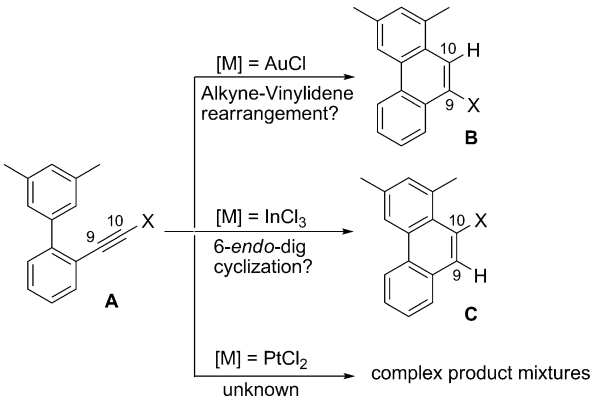

Scheme 1. Transition-metal-catalyzed intramolecular hydroarylation reactions of haloalkynes.

Such regiospecific hydrogen and halogen migrations from halogenated precursors under transition-metal catalysis are useful for the construction of novel products.[20] Previous studies from the Gevorgyan group reported the regioseletive synthesis of 2- and 3-halofurans by gold-catalyzed cycloisomerization of haloallenyl ketones.[21] A later computational and experimental study found that the anionic ligand of gold(I) plays an important role in determining the hydrogen versus halogen migration, by catalyzing the hydrogen migration in a stepwise fashion. Otherwise, the 1,2-halogen migration is more kinetically favorable than the 1,2-hydrogen migration.[7b] In light of these findings and the recent mechanistic studies of H-migration in related systems,[22] we proposed that the reactions discovered by Fürstner et al. could possibly proceed by the detailed mechanisms shown in Scheme 2. Accordingly, from the reactant complex **D**, three pathways, the alkyne–vinylidene rearrangement, 6-*endo*-dig cyclization, and 5-*exo*-dig cyclization, respectively, are possible and could give rise to intermediates ***i***, ***ii***, and ***iii***. While intermediate ***iii*** will exclusively lead to 9-alkylidene fluorene product **E**, which was not obtained in the AuCl- and $InCl_3$-catalyzed reactions, we propose that both the 9-halo- and 10-halophenanthrenes (**B** and **C**, respectively) could be formed from either intermediate ***i*** or intermediate ***ii***.

Thus, a comprehensive study of the mechanisms of the title reactions is desirable for the following reasons. First of all, the pathway by which the $InCl_3$-catalyzed reaction leads to 10-halophenanthrene is unclear. If the 6-*endo*-dig cyclization is more favorable than the other two processes,[13,23] we assumed that the generation of 10-halophenanthrene under $InCl_3$ catalysis is unlikely to result from consecutive 1,2-H migrations from intermediate ***ii***, as after the first 1,2-H migration, the 1,2-halogen migration from intermediate ***iv*** would be more favorable and lead eventually to 9-halophenanthrene.[7b] Most likely, product **C** originates from a 1,3-H shift in intermediate ***ii***, but the pathway by which this process is completed is unknown.

Second, further effort is required to uncover the details of the AuCl-catalyzed reaction. The example of formation of a vinylidene intermediate under gold catalysis is rather rare,[19] and the mechanism in Scheme 2 shows that the 9-halophenanthrene product could also be formed from the 6-*endo*-dig cyclization via intermediates ***ii*** and ***iv***. Although the B3LYP/6-31G* (LANL2DZ) calculations show that the 6-*endo*-dig cyclization is higher in activation energy than the 1,2-Br rearrangement pathway in the AuCl-catalyzed reac-

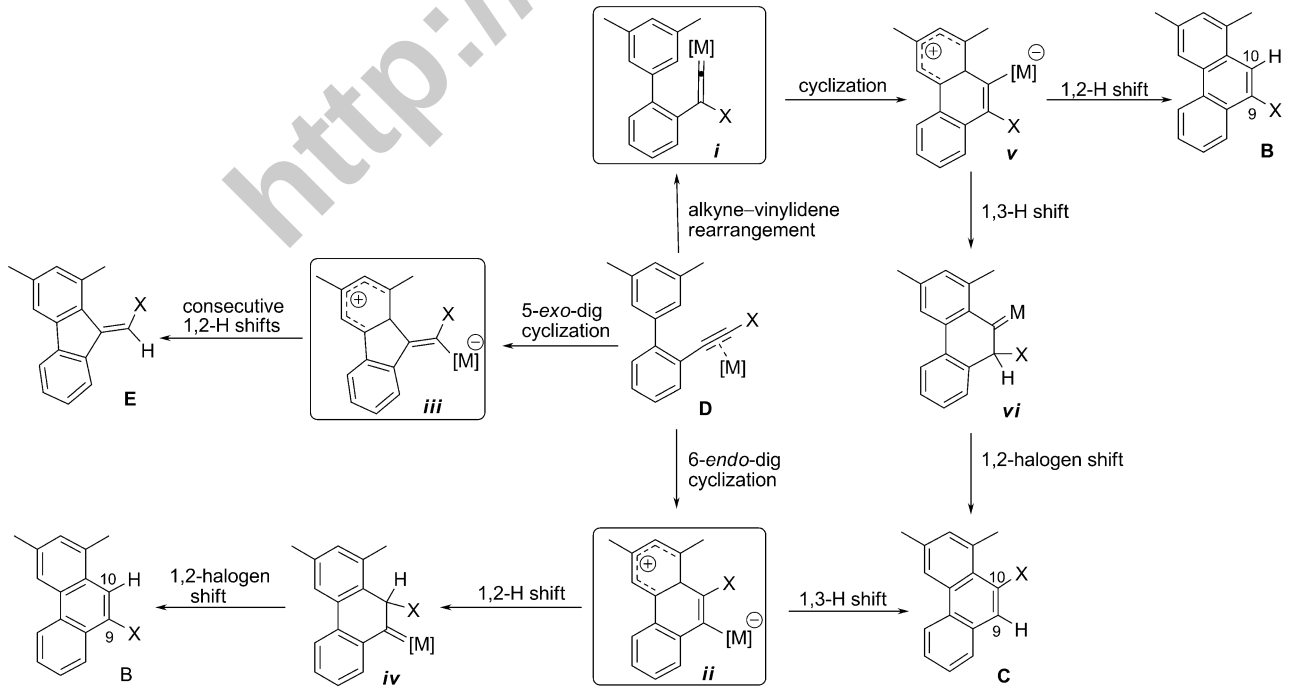

Scheme 2. Possible reaction pathways.

tion,[23] recent studies by Goddard and Toste suggest that alternative functionals may be more accurate for such systems.[24] Validation of the mechanism of the AuCl-catalyzed reaction is necessary.

Third, the origin of the poor selectivity in $PtCl_2$-catalyzed reactions of 2-(haloethynyl)biphenyl derivatives is still unknown.[13] We propose that the product mixtures could result from a competition between the 5-*exo*-dig cyclization, 6-*endo*-dig cyclization, and the 1,2-halogen rearrangement of the reactant complex, or alternatively from the competition of hydrogen versus halogen migration after the formation of intermediates ***i*** and ***ii***. Understanding the poor catalytic performance of $PtCl_2$ in these reactions would provide guidance for the future application of this catalyst in other systems.[25]

To answer the above mechanistic questions, we present, herein, a detailed theoretical study of the transition-metal-catalyzed hydroarylation of halo-alkynes based on calculations by using the DFT-based M06 functional.[26] The computational results give an in-depth understanding of the experimental outcomes found by Fürstner et al.[13,23] All possible 5-*exo*-dig cyclization, 6-*endo*-dig cyclization, and alkyne–vinylidene rearrangement pathways of the bromoalkyne precursor are explored, and the catalyst-dependent selectivity of the reactions is rationalized.[27]

Results and Discussion

$InCl_3$-catalyzed nucleophilic cyclization/intramolecular 1,2-H migration sequence of bromoalkyne 1: To disclose the detailed pathway for formation of 10-halophenanthrene in this system, we first present the DFT-calculated potential-energy surface of $InCl_3$-catalyzed cycloisomerization reactions of model compound **1** in Figure 1, in which all possible intramolecular pathways are included. Geometries of selected intermediates and transition states are given in Figure 2. The relative free energies in toluene (ΔG_{Tol}) show the coordination of $InCl_3$ to **1** is exergonic by 8.6 kcal mol^{-1}, leading to complex **2**. This is a slipped complex with the In–C9 and In–C10 separations being 2.897 and 2.422 Å, respectively (numbering of the atoms is specified in the figures and schemes). As a result of the electrophilic activation by $InCl_3$, complex **2** will undergo Friedel–Crafts-type reactions via transition states **TS1** and **TS1′**, respectively, corresponding to the 6-*endo* and 5-*exo* cyclization processes.[28] In a similar manner

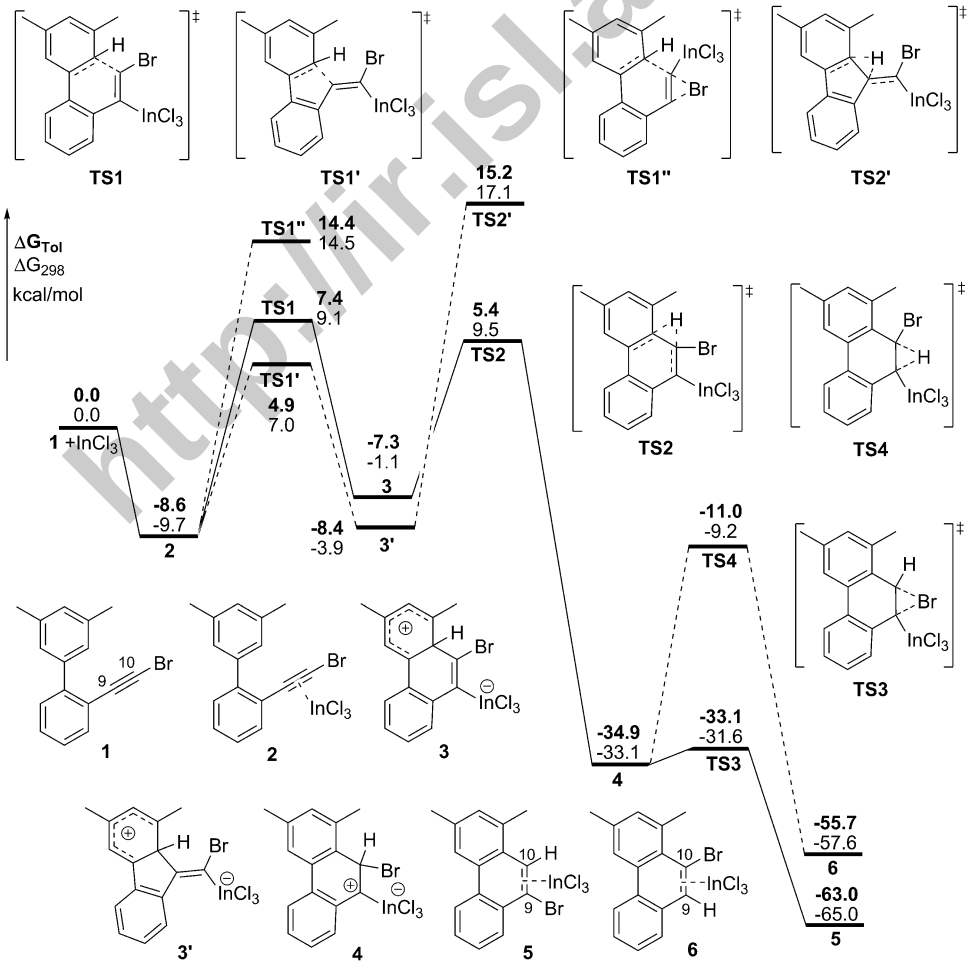

Figure 1. Energy profile for the $InCl_3$-catalyzed cycloisomerization by means of the intramolecular-cyclization/1,2-H-migration sequence.

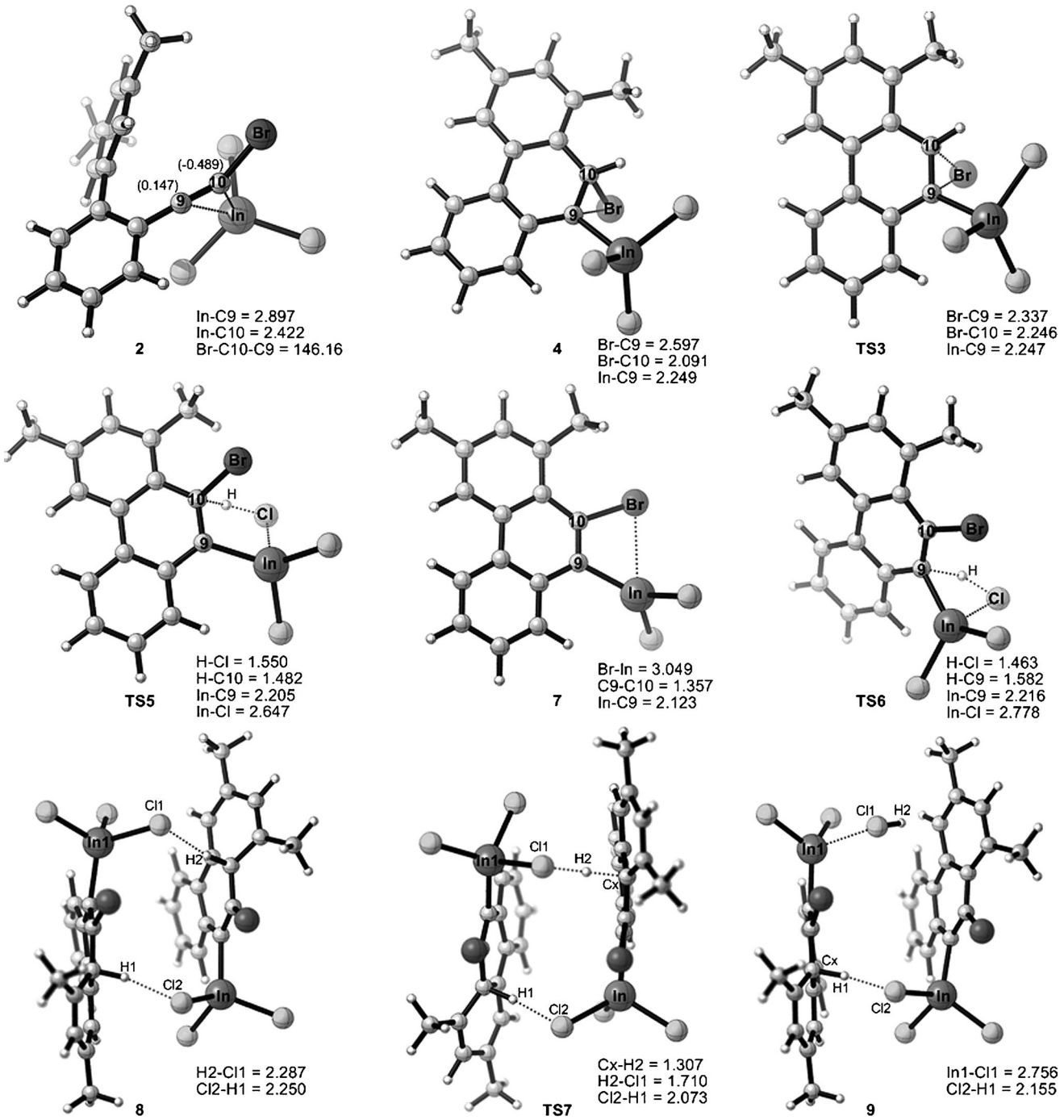

Figure 2. Geometric structures for selected intermediates and transition states in the $InCl_3$-catalyzed reactions. Atomic separations and angles are in Å and °, respectively; values in parenthesis are NPA charges.

to previous calculations,[23] we failed to locate a 1,2-Br migration transition state corresponding to the alkyne–vinylidene rearrangement pathway. Instead, the concerted 1,2-Br migration/cyclization transition-state **TS1″** was found, but this step has a much higher activation barrier than the other two processes. The 5-*exo*-dig cyclization is about 2.5 kcal mol^{-1} lower in activation energy than the 6-*endo*-dig cyclization. This energy difference can be understood by reference to the natural population analysis (NPA) of complex **2**, which shows that the charge populations of C9 and C10 are 0.147 and −0.489, respectively (Figure 2). On overcoming an activation barrier of 13.5 kcal mol^{-1}, the 5-*exo*-dig cyclization leads to intermediate **3′**, which is 0.2 kcal mol^{-1} less stable than **2**. However, the activation free energy for the following 1,2-H shift via **TS2′** is as high as 23.8 kcal mol^{-1} from **2**, making this process unfavorable in comparison with the 6-*endo*-dig cyclization.

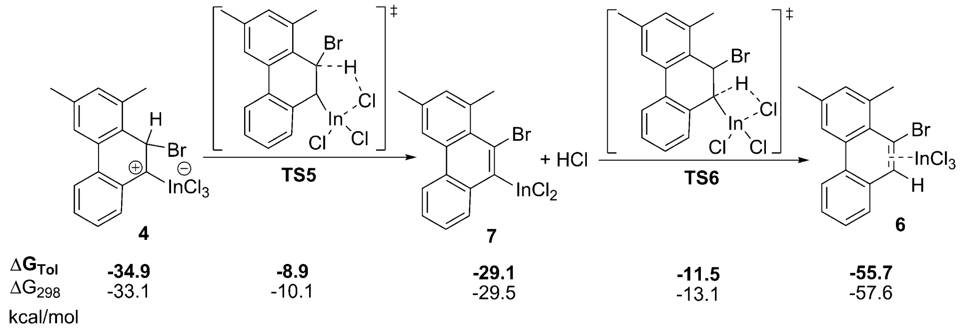

Scheme 3. Possible intramolecular Cl-assisted H-migrations from intermediate **4**.

Through the 6-*endo*-dig cyclization transition-state **TS1**, complex **2** is transformed into Wheland-type intermediate **3** with an activation free energy of 16.0 kcal mol^{-1}. Then from **3**, a zwitterionic intermediate **4** could be formed by an intramolecular 1,2-H migration (**TS2**), which requires an activation free energy of 12.7 kcal mol^{-1}. We considered that **4** is a charge-separated (zwitterionic) species as illustrated in Figure 1, rather than a carbene form, as the In–C9 bond length in **4** is 2.249 Å, which is even slightly longer than that in the alkenyl indium species **3** (2.241 Å). The elongated C10–Br bond length (2.091 Å) and the strong interaction between Br and C9 (C9−Br = 2.597 Å) suggest the positive charge located on C9 in **4** is stabilized by the bromide atom on the neighboring carbon atom (Figure 2). The relative free energy of **4** shows that this intermediate is about 27.6 kcal mol^{-1} more stable than **3**, and the energies of the following transition states (**TS3** and **TS4**) from **4** are much lower than **TS2**. Thus, the formation of **4** is irreversible. As expected, once **4** is generated, the following 1,2-Br migration via **TS3** is almost a barrier-free process, with an activation barrier of only 1.8 kcal mol^{-1} in the toluene solution. This is much more facile than the 1,2-H migration via **TS4**.[7b] The favorable 1,2-Br migration towards C9 is consistent with the geometric structure of **TS3**, which could be reached by only slightly changing the C10–Br and C9–Br separations to 2.246 and 2.337 Å, respectively. The relative free energy will be further decreased to −63.0 kcal mol^{-1} upon formation of **5**, in which $InCl_3$ is loosely associated with the C9=C10 double bond of the 9-bromophenanthrene product (In−C9 = 2.852, In−C10 = 2.772, C9−C10 = 1.374 Å, given in the Supporting Information).

Thus, if the 1,2-H migration (via **TS2**) of Wheland-type intermediate **3** occurs, zwitterionic intermediate **4** will be formed irreversibly, and the eventual formation of 9-bromophenanthrene (from complex **5**) is expected with a facile 1,2-Br migration of **4**. This is completely contrary to the experimental observation that 10-halophenanthrenes were formed selectively in the $InCl_3$-catalyzed reactions.[13]

Possible intramolecular Cl-assisted H-migrations from intermediate 4: Recent works by the groups of Li,[7b] Gevorgyan,[7c] and Ujaque[8c,9d] have disclosed the importance of ligand-assisted H-migrations in gold-catalyzed reactions. Inspired by these findings, we wondered if it is possible to use the Cl ligand of $InCl_3$ as a proton shuttle to transfer the hydrogen atom. To test this idea, we calculated the possible intramolecular Cl-assisted H-migrations from intermediate **4**, and the results are given in Scheme 3. It was found that via hydrogen-abstraction transition-state **TS5**, intermediate **7** and one HCl are formed with an activation free energy of 26.0 kcal mol^{-1}. Intermediate **7** is an aryl indium species in which the C9 of the phenanthrene derivative is substituted by an $InCl_2$ moiety. Clearly, this high-energy process is not possible in competition with the facile 1,2-Br migration via **TS3**. Besides the extremely low activation energy of the 1,2-Br migration, the failure of Cl-assisted H-migration may be attributed to the fused five-membered transition state in this case, as the geometry of **TS5** shown in Figure 2 shows a strong interaction between Cl and In atoms, with a Cl–In separation of 2.647 Å. This result further proves that it is not possible to form the H-migration product (10-halophenanthrene) from intermediate **4**. However, the energy values in Scheme 3 suggest that if the formation of HCl and intermediate **7** occur prior to the formation of **4**, protonation of the In−C9 bond of **7** via **TS6** is expected, as the relative free energy of this four-membered-ring transition state is −11.5, that is, 2.6 kcal mol^{-1} lower than **TS5**. This implies that there should be other possible reaction channels that lead to intermediate **7** and HCl directly from intermediate **2** or **3**.

Intermolecular H-migrations with the assistance of the chloride ligand of $InCl_3$: Considering the increased acidity of the arenium moiety in Wheland-type intermediate **3** and the thermodynamic preference for the formation of **7** and HCl from **3**, we assumed that the deprotonation of **3** by the chloride ligand would be feasible. While the direct dissociations of **3** into charged species were calculated to be energy demanding and no stable ionic pair was found, a favorable intermolecular transformation of **3** into **7** and HCl is depicted in Figure 3.[29]

In this intermolecular H-migration process, H-bonding complex **8** is first formed from two molecules of intermediate **3**. The relative free energies indicate this step is highly favorable, and **8** is formed exergonically by 19.8 kcal mol^{-1} when solvation effects are included. The geometric structure of **8** shows that the two molecules of intermediate **3** are associated together by two C−H···Cl hydrogen-bonding interactions, with the Cl1–H2 and Cl2–H1 separations being 2.287 and 2.250 Å, respectively (Figure 2). Then, via **TS7**, H2 is abstracted by Cl1 with the forming Cl1–H2 and breaking H2–Cx distances being 1.710 and 1.307 Å, respectively. The activation free energy of this step is only 1.3 kcal mol^{-1},

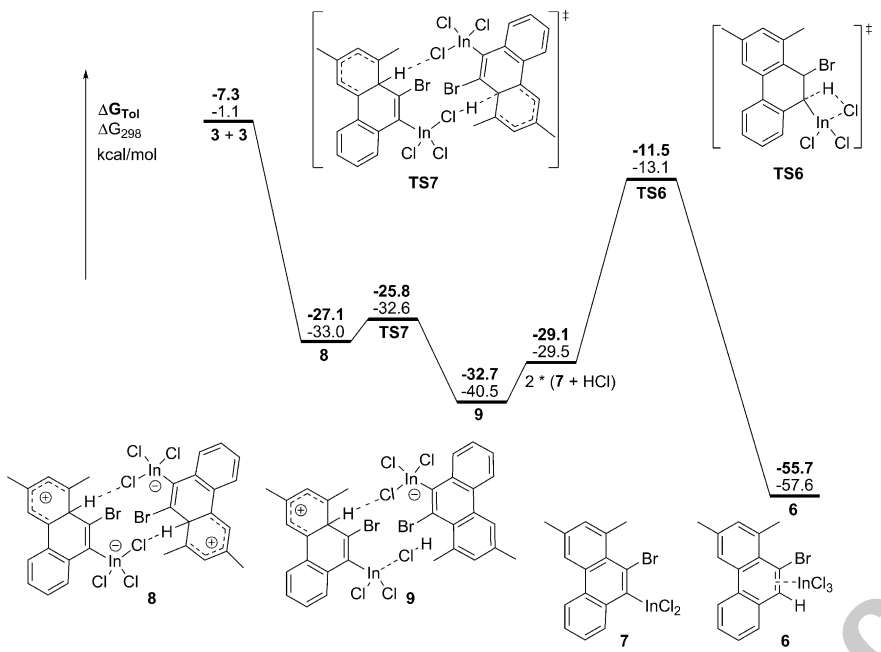

Figure 3. Energy profile for the intermolecular H-migrations of intermediate **3** with the assistance of a Cl ligand.

which indicates the intermolecular H-abstraction by the chloride ligand is very facile. The geometry shows that the Cl2–H1 separation is slightly reduced to 2.073 Å in **TS7**. The intrinsic reaction coordinate (IRC) analysis of **TS7** indicates that the intermolecular H-migrations are completed in a stepwise fashion, and the resulting zwitterionic intermediate from **TS7** is **9**, which is 5.6 kcal mol^{-1} more stable than complex **8**. In **9**, the Cl2–H1 separation is 2.155 Å, and the Cx–H1 bond is significantly weakened, as shown by the clearly elongated Cx–H1 bond length of 1.160 Å (Figure 2). All attempts to locate a second H-migration transition state to transfer H1 from Cx to Cl2 failed. This may be attributed to the instability of **9** and the very small barrier of this step, as a slight shortening of the Cl2–H1 separation or removal of H2–Cl1 from **9** would result in transferring H1 to Cl2 directly. The energies indicate that the dissociation of **9** into two of **7** and of HCl requires a reaction free energy of about 3.6 kcal mol^{-1}. Thus, Figure 3 shows that the intermolecular formation of **7** and HCl from **3** are favorable kinetically. Finally, product complex **6**, the complex of $InCl_3$ and 10-bromophenanthrene, is formed by proto-demetalation of **7**. This step is completed via transition state **TS6**, from which the hydrogen of HCl is donated to C9 and the $InCl_3$ catalyst is regenerated. This final step also represents the rate-limiting step of the $InCl_3$-catalyzed reaction, with an activation barrier of 21.2 kcal mol^{-1} from **9**. Thus, in the $InCl_3$-catalyzed reactions, the retention of the halogen on C10 of the product is attributed to the intermolecular hydrogen shifts of two Wheland-type intermediates with the assistance of the chloride ligand; otherwise, the halogen migration product would be expected.

Validation of the computational method for the AuCl-catalyzed reaction: Although the 10-halophenanthrene product in the AuCl-catalyzed reaction was thought to originate from the AuCl-catalyzed 1,2-halogen rearrangement of the haloalkyne, Scheme 2 shows that the 10-halophenanthrene product could be formed from both the alkyne–vinylidene rearrangement and the 6-*endo*-dig cyclization pathways. To uncover which one is more favorable, energies from different computational methods are compared to ascertain the initiation of the AuCl-catalyzed reaction (Table 1).

The results suggest that the relative energies for the 6-*endo* cyclization (**TS1″-Au**) and the 1,2-Br rearrangement (**TS1-Au**) processes under AuCl catalysis are computational-method dependent. In line with a previous study,[23] the calculations by the B3LYP/6-31G* (LANL2DZ for Au and Br) method predict that the alkyne–vinylidene rearrangement through a 1,2-Br migration (**TS1″-Au**) is the more favorable by 6.7 kcal mol^{-1}. To test the reliability of the B3LYP energy, however, single-point calculations at the MP2/6-31+G**//B3LYP/6-31G* (LANL2DZ for Au and Br) level found that **TS1-Au** is more favored by 4.3 kcal mol^{-1}. The preference of the 6-*endo*-dig cyclization is further validated by the relative free energies from the MP2/6-31G* (LANL2DZ for Au and Br) geometry optimizations and frequency calculations. Interestingly, the recently developed DFT-based M06 functional (M06/6-31+G** (LANL2DZ for Au and Br)) reproduces the energetic scenario of MP2 calculations, albeit a smaller energy gap is obtained. The M06 method has lately been proven to provide good accuracy for the estimation of barrier heights involving transition metals.[24,26] Thus, for reliability and efficiency reasons, the detailed pathways for the AuCl-catalyzed reaction of **1** by the M06 method are depict-

Table 1. Relative free energies for the AuCl-catalyzed 6-*endo*-dig cyclization (**TS1-Au**) and alkyne–vinylidene rearrangement (**TS1″-Au**) pathways of **1** at different levels of theory.

Transition state	Relative energy [kcal mol^{-1}]			
	B3LYP[a]	MP2//B3LYP[b]	MP2[c]	M06[d]
TS1-Au	6.7	−4.3	−2.4	−1.6
TS1″-Au	0.0	0.0	0.0	0.0

[a] B3LYP/6-31G* (LANL2DZ) with CPCM correction. [b] MP2/6-31+G* (LANL2DZ)//B3LYP/6-31G* (LANL2DZ). [c] MP2/6-31G* (LANL2DZ). [d] M06/6-31+G** (LANL2DZ) with CPCM correction.

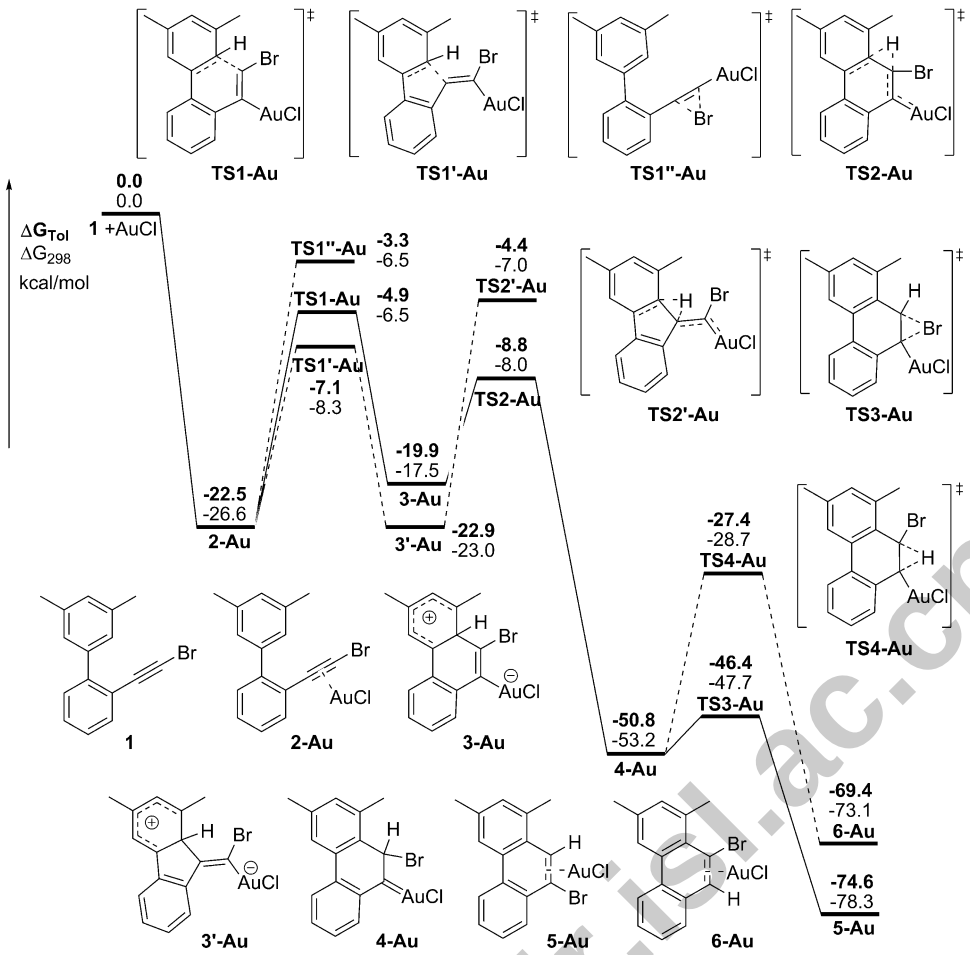

Figure 4. Potential-energy surface for the AuCl-catalyzed reaction.

ed in Figure 4, and the geometric structures of selected intermediates and transition states are collected in Figure 5. Despite the accuracy problem, the B3LYP and M06 results show these intriguing experimental observations may be explained by different mechanisms.[30]

Formation of 9-halophenanthrene through a AuCl-catalyzed 6-*endo*-dig cyclization: According to the results provided in Figure 4, the first coordination of AuCl to the alkyne moiety of **1** to form complex **2-Au** is exergonic by 22.5 kcal mol^{-1}. The geometric structure of the slipped complex **2-Au** suggests that AuCl strongly interacts with both C9 and C10 of **1**, with Au–C9 and Au–C10 separations being 2.303 and 2.119 Å (Figure 5), respectively. Then, from **2-Au**, the energy of the alkyne–vinylidene rearrangement pathway through a 1,2-Br migration (**TS1″-Au**) is the highest, being 3.8 and 1.6 kcal mol^{-1} higher than the 5-*exo*-dig cyclization (**TS1′-Au**) and 6-*endo* cyclization (**TS1-Au**), respectively. The activation energy of the 5-*exo*-dig cyclization (**TS1′-Au**) is 15.4 kcal mol^{-1}, and intermediate **3′-Au** is formed slightly exergonically, by 0.4 kcal mol^{-1} in toluene solution. However, this step is reversible due to the free energy of the following 1,2-H migration transition-state **TS2′-Au**, which is 2.7 kcal mol^{-1} higher than **TS1′-Au**. Further calculations indicate that the 1,2-H step (via **TS2′-Au**) will be irreversible, as the generated intermediate (not shown) will be 16.7 kcal mol^{-1} more stable than **3′-Au**. Thus, the 5-*exo*-dig cyclization selectivity is determined by the energy gap between **3′-Au** and **TS2′-Au**, which is 18.5 kcal mol^{-1}. This energy gap is 0.9 kcal mol^{-1} higher than the energy gap between **2-Au** and **TS1-Au**, which determines the activation energy of the 6-*endo*-dig cyclization. This is in qualitative agreement with the fact that no 9-alkylidene fluorene derivative was observed in experiments, and suggests that the AuCl-catalyzed 6-*endo* cyclization via **TS1-Au** is the major reaction channel.

Through the 6-*endo*-dig cyclization pathway, **2-Au** is transformed endogonically into the Wheland-type intermediate **3-Au**. The relative instability of this zwitterionic intermediate may be caused in part by the steric repulsion between the bromide on C10 and the methyl on C1. This is shown by the twisted geometry of **3-Au**, in which the Br-C10-C1-Me, Br-C10-C9-Au, and Br-C10-C9-Cy dihedral angles are 40.87, −15.35, and 160.44°, respectively.[31] After cyclization to **3-Au**, the following 1,2-H shift via **TS2-Au** requires an activation free energy of 11.1 kcal mol^{-1}, leading irreversibly to gold carbenoid **4-Au**, which is 50.8 kcal mol^{-1} lower in free energy than the free reactant. Presumably, the kinetic and thermodynamic preference of carbenoid **4-Au** over **3-Au** is driven forward by the re-establishment of the aromaticity. Furthermore, carbenoid **4-Au** could also be stabilized by both the effect of the bromine atom at C10 (C10−Br = 2.082 and C9−Br = 2.712 Å) and the relativistic effect of gold.[1o] In **4-Au**, the Au–C9 bond length is 1.994 Å, which is only 0.066 Å shorter than the length in the alkenyl gold species **3-Au**, which suggests intermediate **4-Au** is close to a gold-stabilized cation.[32] However, this distance is also quite close to the Au=C separations in other gold carbene species.[24c] As expected, the 1,2-Br shift (via **TS3-Au**) from intermediate **4-Au** is much more facile, being 19.0 kcal mol^{-1} lower in activation energy than the 1,2-H shift (via **TS4-Au**). Thus, product complex **5-Au** from the 1,2-Br shift is favored both kinetically and thermodynamically. Accordingly, Figure 4 shows that after the AuCl-catalyzed 6-*endo*-dig cyc-

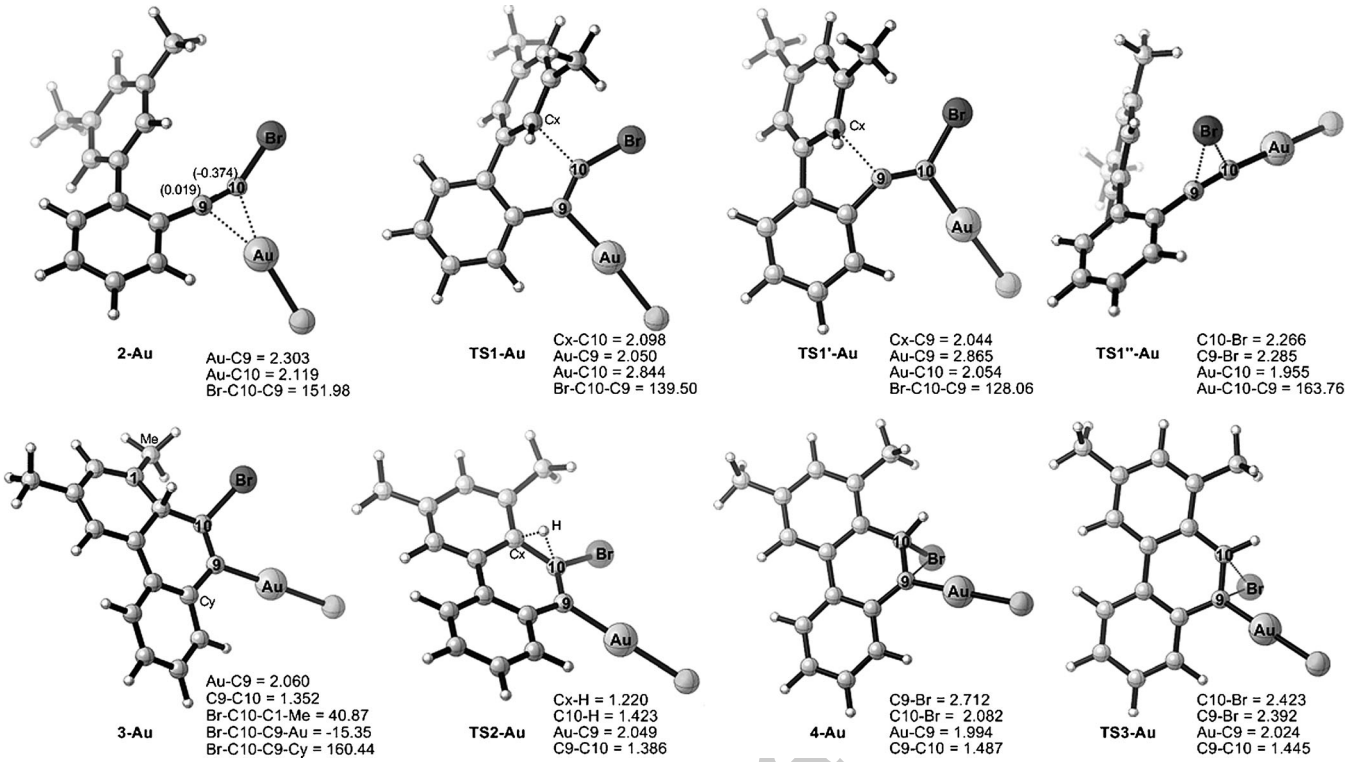

Figure 5. Geometric structures for selected intermediates and transition states in the AuCl-catalyzed reaction. Atomic separations and angles are in Å and °, respectively; values in parenthesis are NPA charges.

lization of **1**, the 9-halophenanthrene product could be formed by consecutive 1,2-H/1,2-halogen migrations, instead of passing through the vinylidene intermediate.

Possible initiations of the $PtCl_2$-catalyzed reaction: To provide guidance for future design, the cause of the poor selectivity of the $PtCl_2$ catalyst in the experiments by the Fürstner group was explored to determine what product mixtures might be formed.[13a] Likewise, the relative energies and selected structural parameters of the three possible transition states starting from reactant complex **2-Pt** are depicted in Scheme 4. Besides the relatively lower activation energies of these steps in comparison with the corresponding barriers in the $InCl_3$- and AuCl-catalyzed reactions, one notable difference is that the 1,2-Br rearrangement in the $PtCl_2$-catalyzed reaction is comparable to the Friedel–Crafts cyclization.[33] The energy values show that the $PtCl_2$-catalyzed 6-*endo*-dig cyclization (**TS1-Pt**) is the most difficult with a highest activation barrier of 14.6 kcal mol^{-1}, and the activation free energies of the 1,2-Br rearrangement (**TS1″-Pt**) and 5-*exo*-dig cyclization (**TS1′-Pt**) are quite close at 13.1 and 12.9 kcal mol^{-1}, respectively. Whereas the higher energy of **TS1-Pt** than **TS1′-Pt** could be attributed to the electronic (the NPA charges on C9 and C10 of **2-Pt** are 0.161 and −0.289, respectively) and steric factors, the relative low barriers of the 1,2-Br rearrangement and the 5-*exo*-dig cyclization under $PtCl_2$ catalysis, in comparison with the AuCl- and $InCl_3$ cases, could be better understood by structural analysis of the reactant complexes.

As shown in Scheme 4, the two extreme mesomeric forms of the reactant complexes could be represented as **M1** and **M2**.[2b] In complex **2-Pt**, the Pt is bound much more strongly to C10 than to C9, and the Pt–C10 separation of 1.960 Å is even shorter than the lengths of typical Pt–C single bonds.[34] In the AuCl counterpart, the Au is strongly bound to both C9 and C10 in **2-Au** (Figure 5). Thus, the activation of alkyne **1** by $PtCl_2$ should be depicted as the zwitterionic form **M2**, whereas **2-Au** more closely resembles the π-complex form of **M1** (Scheme 4). This is also implied by the increased positive charge on C9 and greater bending of the alkyne moiety (Br-C10-C9 angle is 138.11°) in **2-Pt** than in **2-Au**. Presumably, the relativistically expanding 5d orbitals of Pt might stabilize the positive charge on C9 of **2-Pt**, which exhibits a Pt–C9 separation of 2.406 Å. The interaction of alkyne **1** with $InCl_3$ (formation of **2**, Figure 2) resembles **2-Pt**; however, the poor backbonding ability of this harder Lewis acid only activates the alkyne to a limited extent, as shown by the lower exergonicity for formation of **2** (Figure 1) and the larger In–C9 and In–C10 separations (Figure 2) and the smaller charge transfer in this complex (see below). The lack of back-donation from indium also blocks the formation of a stable vinylidene complex, and thus, no transition state for such a process could be located. The charge transfers from the substrate moiety to the metal chloride unit in **2**, **2-Au**, and **2-Pt** are −0.119, 0.009, and −0.341, respectively. The small positive charge transfer from **1** to AuCl in **2-Au** suggests strong back-donation of Au d electrons into the antibonding orbital of the alkyne, and ren-

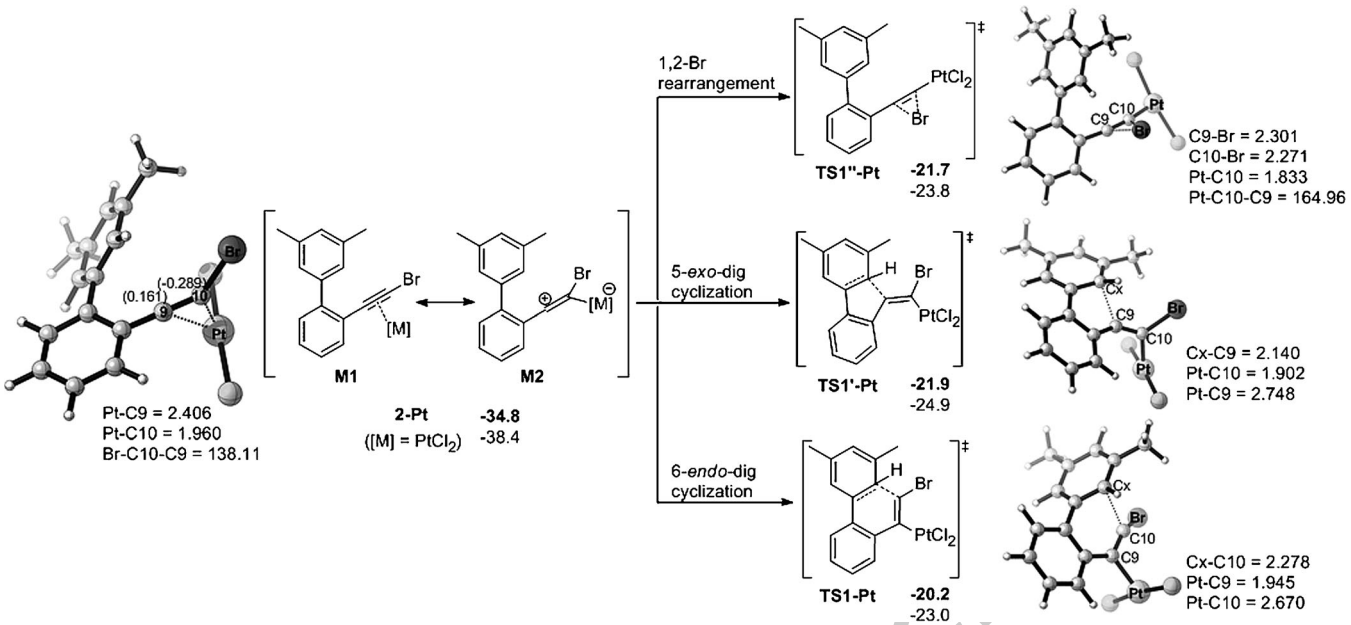

Scheme 4. Relative free energies (in kcal mol^{-1}) in toluene solution (ΔG_{Tol}, bold) and in the gas phase (ΔG_{298}, plain) for the 1,2-Br rearrangement, 5-*exo*-dig cyclization, and 6-*endo*-dig cyclization transition states in the $PtCl_2$-catalyzed reaction. Atomic separations and angles are in Å and °, respectively; values in parenthesis are NPA charges.

ders the substrate moiety more electron abundant. This in turn makes **2-Au** the most difficult complex to undergo Friedel–Crafts cyclizations and the 1,2-Br rearrangement among the three reactant complexes. In summary, as a result of the subtle interplay of steric and electronic factors, coordination of bromoalkyne **1** to $PtCl_2$ forms a zwitterionic complex **2-Pt**, which has a more electrophilic C9 atom and enables more facile 5-*exo*-dig cyclization and 1,2-Br rearrangement, accounting for the calculated energy values.

In the $InCl_3$ and AuCl sections we have disclosed that the 5-*exo*-dig cyclization steps in these cases are reversible, due to the fact that the 1,2-H shift transition state is higher in energy than the 5-*exo*-dig cyclization transition state. However, in the $PtCl_2$-catalyzed reaction, the 5-*exo*-dig intermediate is formed exergonically from **2-Pt**, and the energy of the subsequent 1,2-H shift transition state will be relatively lower than **TS1′-Pt**, as will be described later. Thus, both the alkyne–vinylidene rearrangement and 5-*exo*-dig cyclization pathways are the possible reaction channels in the $PtCl_2$-catalyzed reaction. The detailed mechanisms leading to the final products from these two processes are presented below, which suggest that all three products, that is, 9-bromophenanthrene, 10-bromophenanthrene, and 9-alkylidene fluorene, are possible in the $PtCl_2$-catalyzed reaction of **1**.

Details for the $PtCl_2$-catalyzed alkyne–vinylidene rearrangement pathway: The potential-energy surface of this pathway is shown in Figure 6, and the geometric structures of selected intermediates and transition states are depicted in Figure 7. As mentioned above, the first step of this mechanism is a 1,2-Br migration via **TS1″-Pt**, which converts complex **2-Pt** into Pt–vinylidene intermediate **3″-Pt**,[33] with the free energy increased by 3.7 kcal mol^{-1}. Complex **3″-Pt** is an almost linear complex with the Pt-C10-C9 angle at 171.30°. The Pt–C10 bond length in **3″-Pt** is 1.785 Å, which is slightly shorter than the length of a Pt=C double bond[35] and features a multiple Pt–C bond between double and triple.[36] In the following step, cyclization of **3″-Pt** into Wheland-type intermediate **4″-Pt** is expected, although we failed to locate the cyclization transition state (**TS″**) with the M06 functional, possibly due to the very reactive nature of vinylidene complex **3″-Pt**, as calculations at the B3LYP/6-31G* (LANL2DZ) level found the activation energy of this step is only about 0.6 kcal mol^{-1}. In **4″-Pt**, the $PtCl_2$ is connected to C10 with a Pt–C10 bond length of 1.938 Å, and the positive charge on the arenium ion moiety is stabilized by one of the chloride ligands, with the Cl–H and H–Cx separations at 2.325 and 1.151 Å, respectively. Then, from intermediate **4″-Pt**, a 1,2-H shift transition state was located as **TS2″-Pt**, which would lead to complex **6″-Pt** with an activation energy of 10.0 kcal mol^{-1}.

However, instead of undergoing the above low-energy 1,2-H shift step via **TS2″-Pt**, the chloride of the $PtCl_2$ moiety in intermediate **4″-Pt** can act as a base to abstract the hydrogen to be shifted via **TS3″-Pt**, and this latter deprotonation process is much more facile with an activation barrier of only 2.7 kcal mol^{-1}. In **TS3″-Pt**, the Cl–H and H–Cx separations are changed to 1.758 and 1.295 Å, respectively, and the Pt–Cl bond is only slightly elongated to 2.431 from 2.375 Å in **4″-Pt** (Figure 7), which indicates a small geometry change to reach the transition state. Thus, the deprotonated intermediate **5″-Pt** is formed kinetically. In **5″-Pt**, the HCl moiety is associated with the Pt atom by Pt···Cl interaction with a further elongated Pt–Cl separation of

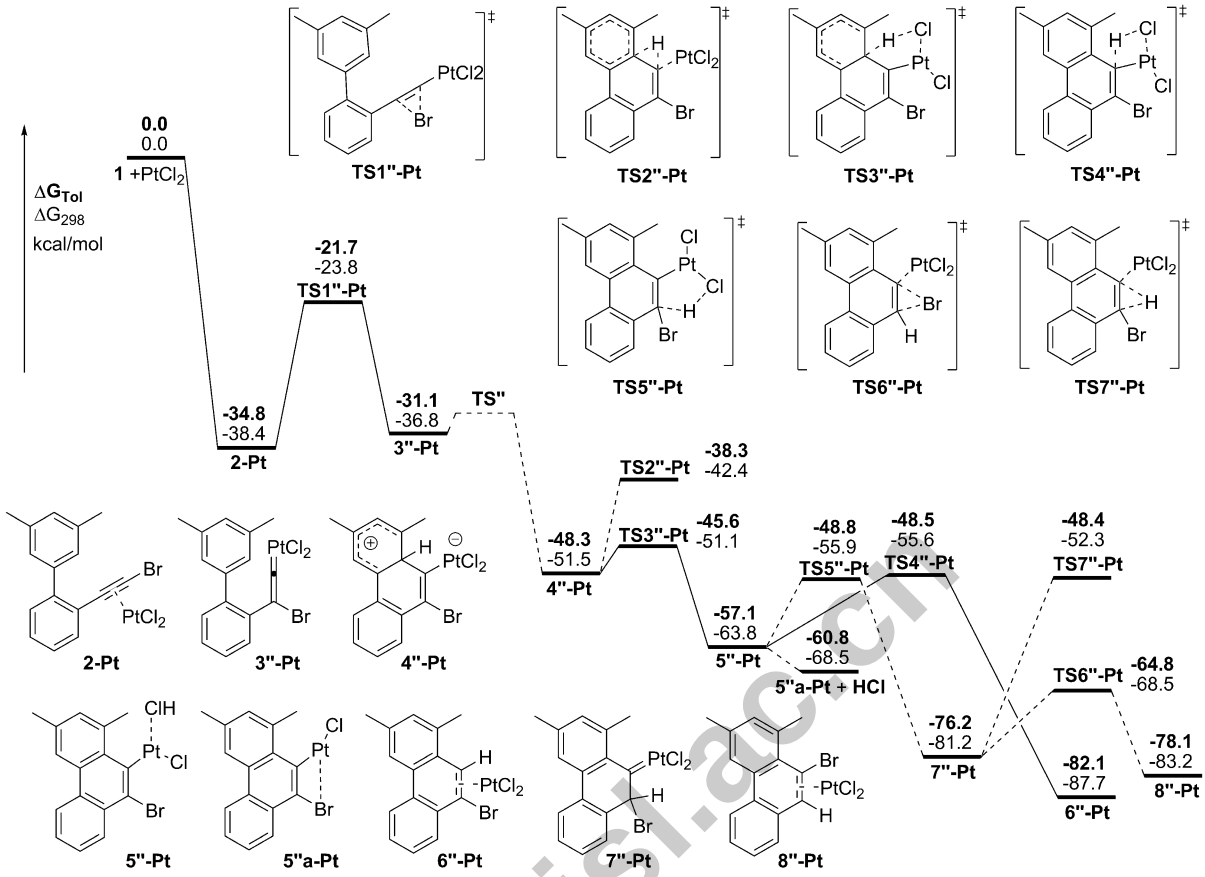

Figure 6. Detailed mechanism for the $PtCl_2$-catalyzed alkyne–vinylidene rearrangement pathway.

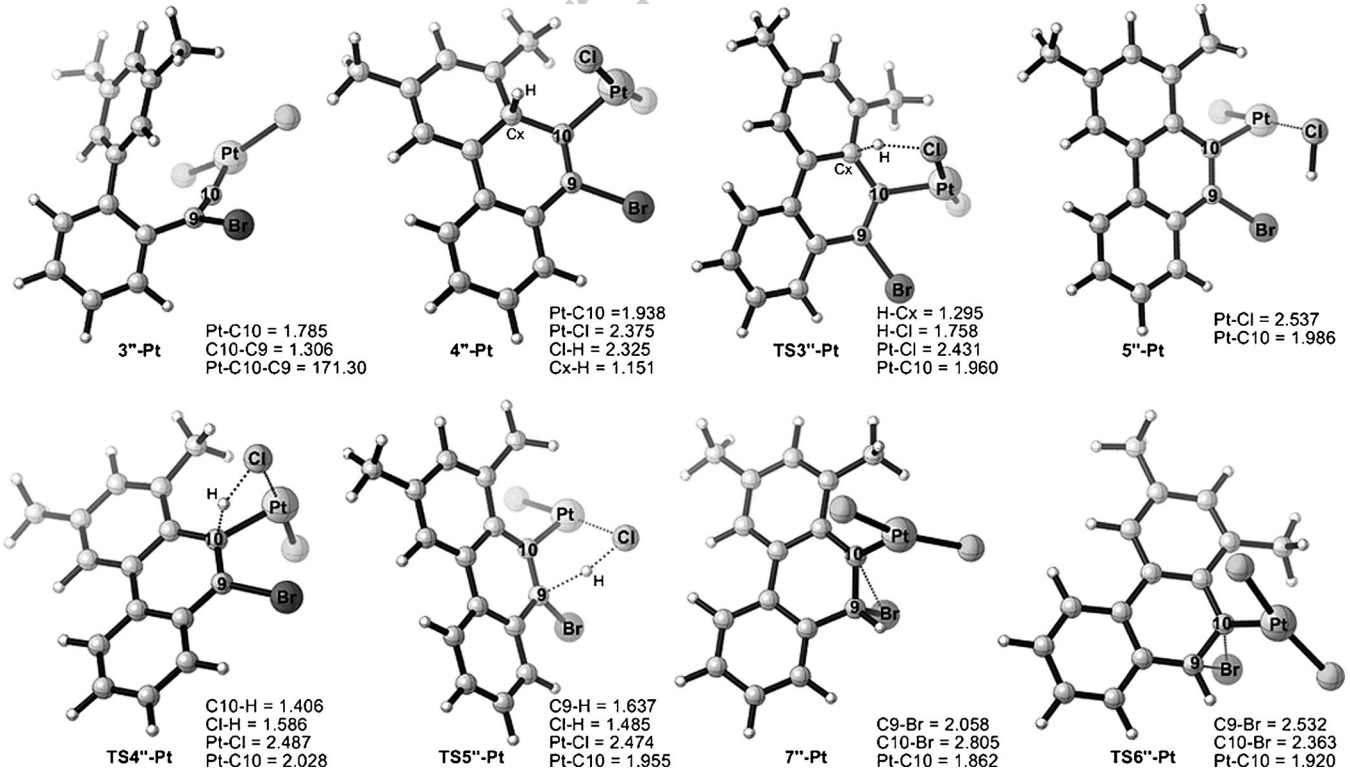

Figure 7. Geometric structures for selected intermediates and transition states in the $PtCl_2$-catalyzed alkyne–vinylidene pathway. Atomic separations and angles are in Å and °, respectively; values in parenthesis are NPA charges.

2.537 Å. Complex **5″-Pt** could equilibrate into **5″a-Pt** and HCl with an exergonicity of 3.7 kcal mol^{-1}. From **5″-Pt**, the protonation of either C10 or C9 by HCl is possible, as the two transition states, **TS4″-Pt** and **TS5″-Pt**, respectively, are nearly the same energy. Through the four-membered-ring transition-state **TS4″-Pt**, the proto-demetalation reaction occurs by passing a barrier of 8.6 kcal mol^{-1}. In this transition state, the C10–H and H–Cl separations are 1.406 and 1.586 Å, respectively. This step leads to product complex **6″-Pt** highly exergonically, and the 9-bromophenanthrene product will be generated by decomplexation of the $PtCl_2$ catalyst from **6″-Pt**. Alternatively, **TS5″-Pt** is a five-membered-ring transition state and is 0.3 kcal mol^{-1} lower in energy than **TS4″-Pt**. Through **TS5″-Pt**, the hydrogen is donating to C9, with the C9–H and H–Cl separations at 1.637 and 1.485 Å, respectively. The generated intermediate **7″-Pt** could be depicted as a carbene-like intermediate,[35] as the Pt–C10 bond length is 1.862 Å, which is significantly shorter than the length of a Pt–C single bond.[34] The bromide on C9 also interacts with C10 agostically (C10–Br = 2.805 and C9–Br = 2.058 Å), but to a smaller extent than in analogues **4** (Figure 2) and **4-Au** (Figure 5). This intermediate is also unstable towards 1,2-Br migration via **TS6″-Pt**, which requires an activation barrier of 11.4 kcal mol^{-1} and leads to **8″-Pt**, a π-complex of $PtCl_2$ and 10-bromophenanthrene. The 1,2-H shift of **7″-Pt** via **TS7″-Pt** is unfavorable, having a much higher energy. Thus, both 9- and 10-bromophenanthrene products are expected in the $PtCl_2$-catalyzed alkyne–vinylidene rearrangement of **1** because in the chloride-assisted H-migrations, the protonations of either C9 or C10 in intermediate **5″-Pt** have almost of the same probability.

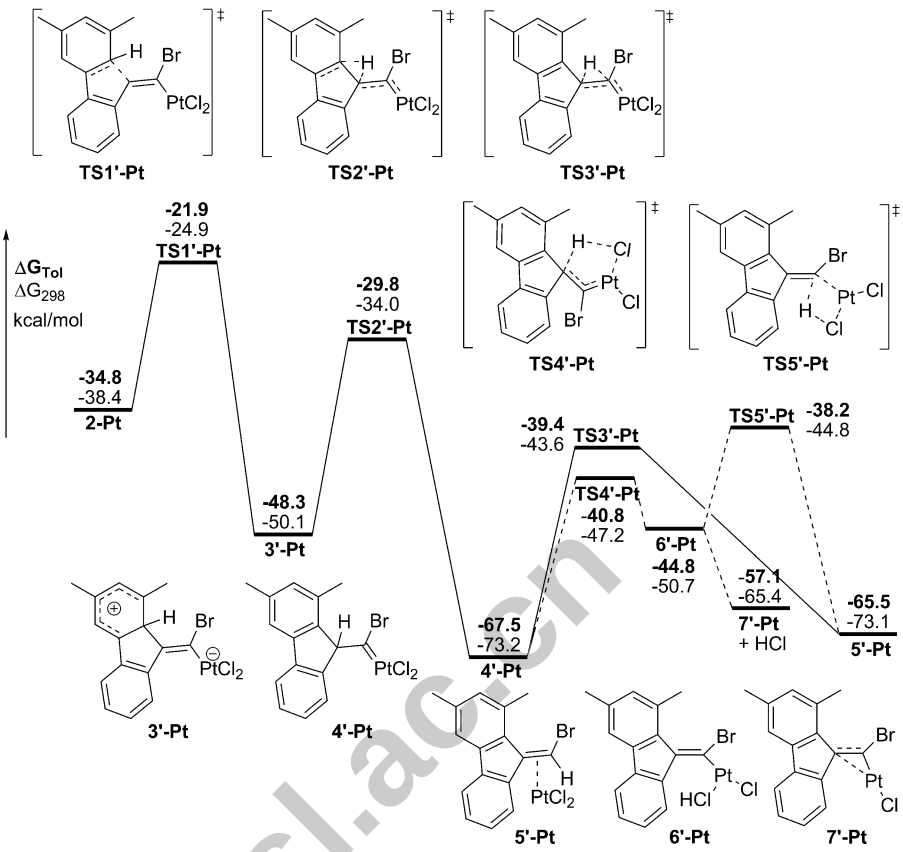

Figure 8. Detailed mechanism for the $PtCl_2$-catalyzed 5-*exo*-dig cyclization pathway.

Details for the $PtCl_2$-catalyzed 5-*exo*-dig cyclization pathway: As mentioned previously and shown by the potential energy surface in Figure 8, by passing through the 5-*exo*-dig cyclization transition-state **TS1′-Pt**, complex **2-Pt** is transformed into intermediate **3′-Pt**. This step is different from the $InCl_3$- and AuCl-catalyzed 5-*exo*-dig cyclizations, as both the conversion of **2** to **3′** (Figure 1) and **2-Au** to **3′-Au** (Figure 4) are almost energetically neutral processes, whereas **3′-Pt** is more energetically favorable than **2-Pt** by 13.5 kcal mol^{-1}. The higher relative energies of the 1,2-H shift transition-states **TS2′** and **TS2′-Au** make the $InCl_3$- and AuCl-catalyzed 5-*exo*-dig cyclizations reversible and unfavorable. However, as Figure 8 shows, **TS2′-Pt**, the 1,2-H shift transition state from **3′-Pt**, is 7.9 kcal mol^{-1} lower in energy than **TS1′-Pt**. Thus, the formation of **3′-Pt** is irreversible because the forward reaction via **TS2′-Pt** would be much easier than the reverse reaction via **TS1′-Pt**, although the 18.5 kcal mol^{-1} activation energy is the same as the activation energy of this type of 1,2-H shift, **TS2′-Au**, shown in Figure 4. This implies the importance of the stability of the **3′-Pt**-like intermediate relative to the reactant complex on determining the 5-*exo*-dig cyclization selectivity. Structural analysis indicates that the steric repulsion between the bromide atom and the methyl group on C1 in **3′-Pt** is the least of the three analogues, as revealed by the largest Br-C10-C1-Me dihedral angle of 66.02° in **3′-Pt** (Figure 9), in comparison with the dihedral angle values of 63.85 and 62.71° in **3′** and **3′-Au**, respectively.

The 1,2-H shift of **3′-Pt** leads to a Pt–carbene intermediate **4′-Pt** (Pt–C10 = 1.824 Å, Figure 9) irreversibly, with an overall exergonicity of 32.7 kcal mol^{-1} from **2-Pt**. Complex **4′-Pt** represents the global free-energy minimum on the potential-energy surface, and it is relatively stable against further hydrogen shifts. The direct 1,2-H shift via **TS3′-Pt** requires an activation free energy of 28.1 kcal mol^{-1}, and product complex **5′-Pt** is 2.0 kcal mol^{-1} less stable than **4′-Pt**. Cal-

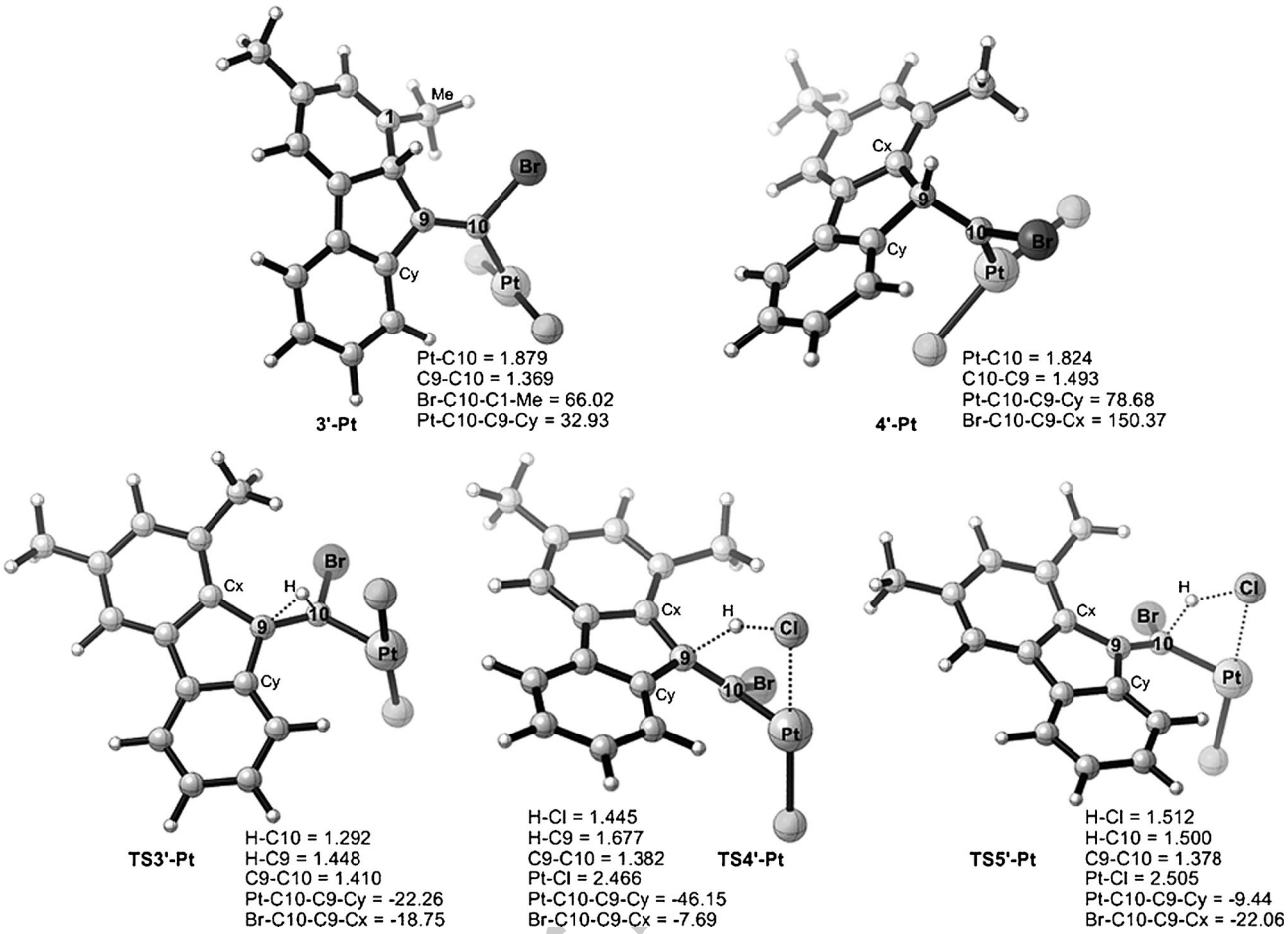

Figure 9. Geometric structures for selected intermediates and transition states in the $PtCl_2$-catalyzed 5-*exo*-dig cyclization pathway. Atomic separations and angles are in Å and °, respectively.

culations indicate the chloride of $PtCl_2$ could also facilitate this 1,2-H shift, transforming it into a stepwise process; however, the activation free energy will be increased by about 1.2 kcal mol^{-1}. First, H-abstraction by the chloride occurs via **TS4′-Pt**. This step requires an activation free energy of 26.7 kcal mol^{-1}, and gives rise to intermediate **6′-Pt**, which is 22.7 kcal mol^{-1} more unstable than **4′-Pt**. The dissociation of HCl from **6′-Pt** is possible, but the free energy sum of HCl and intermediate **7′-Pt** is 10.4 kcal mol^{-1} higher than **4′-Pt**. To complete the chloride-assisted hydrogen shift, in the second step, conversion of **6′-Pt** into complex **5′-Pt** could be realized by H-donation from HCl via **TS5′-Pt**. Due to the reversibility of the H-abstraction step, the activation free energy of this stepwise process is determined by the energy gap between **4′-Pt** and **TS5′-Pt**, which is 29.3 kcal mol^{-1}. Thus, the last step, the 1,2-H shift from Pt–carbene **4′-Pt** is the most difficult in the $PtCl_2$-catalyzed 5-*exo*-dig cyclization pathway.

The high activation energies of both the 1,2-H shift and the chloride-assisted H-shifts from carbene **4′-Pt** should be attributed to the late nature of the transition states. In **TS3′-Pt**, **TS4′-Pt**, and **TS5′-Pt**, the C9=C10 double bonds are substantially formed (Figure 9). The evident product-like character of these transition states agrees with the reaction endergonicity, as predicted by the Hammond postulate.[37] Hence, the high activation energies calculated for these H-shifts correspond to the large geometry changes between **4′-Pt** and the transition states.

Conclusion

A comprehensive DFT/M06 study of the transition-metal-catalyzed hydroarylation of the 2-(haloethynyl)biphenyl derivatives of Fürstner et al.[13] was carried out by using the bromoalkyne as a model reactant, and all possible 5-*exo*-dig cyclization, 6-*endo*-dig cyclization, and alkyne–vinylidene rearrangement pathways are compared to understand the observed divergence of the $InCl_3$, AuCl, and $PtCl_2$-catalyzed reactions.

The results revealed that both the $InCl_3$ and AuCl catalysts favor the 6-*endo*-dig cyclization, and the formations of 9-bromo- and 10-bromophenanthrenes from the AuCl and $InCl_3$ catalysis, respectively, originate from different H-migration pathways of the generated Wheland-type intermediates. In the AuCl case, the facile 1,2-H/1,2-Br migration se-

quence of **3-Au** leads to the 9-bromophenanthrene product exclusively. However, for intermediate **3** of the $InCl_3$-catalyzed 6-*endo* cyclization, the intermolecular deprotonation of two molecules of intermediate **3** into two aryl indium species and HCl is more favorable than the 1,2-H shift. Then, the proto-demetalation of the aryl indium species by HCl gives rise to 10-bromophenanthrene. Thus, the retention of the bromide on C10 in the $InCl_3$-catalyzed reaction is attributed to the intermolecular hydrogen shifts with the assistance of the chloride ligand.

The predictions for the $PtCl_2$-catalyzed reactions are consistent with the poor selectivity in $PtCl_2$ catalysis. Both the $PtCl_2$-catalyzed alkyne–vinylidene rearrangement and the 5-*exo*-dig cyclization are favorable with activation energies of around 13.0 kcal mol^{-1}. In the alkyne–vinylidene rearrangement pathway, interesting Cl-assisted H-migrations were observed, and the protonations of the C10–Pt and C9–Br bonds by HCl are very close in energy, leading eventually to both the 9- and 10-bromophenanthrenes with similar kinetic preference. Alternatively, the 5-*exo*-dig cyclization intermediate could be transformed irreversibly into a Pt–carbene intermediate from a first 1,2-H shift, then, the formation of a 9-alkylidene fluorene derivative is possible by a second 1,2-H shift, but a relatively high energy barrier accompanies the transformation.

In summary, this computational study provides a better understanding of the experiments of Fürstner et al.,[13,23] sheds new light on the subtle differences between the $InCl_3$, AuCl, and $PtCl_2$ catalysts as alkyne activators,[1–5] and demonstrates the important role of the chloride ligand of the metal catalyst in intra- and intermolecular H-migrations.[7,22]Moreover, the results validate the M06 functional as a reliable method for mechanistic simulation of $InCl_3$, AuCl, and $PtCl_2$ catalysis. All these should have implications for the design of novel transition-metal-catalyzed alkyne transformations and reactions through selective hydrogen versus halogen migration.[38]

Computational Details

Computational methods: All of the calculations were carried out with the Gaussian 09 suite of computational programs.[39] The geometries of all stationary points were optimized at the DFT level by using the M06 hybrid functional.[40] The standard 6-31+G** basis set[41] has been applied for all the atoms except Br, In, Au, and Pt, which have been described by the LANL2DZ basis set.[42] Frequencies were analytically computed at the same level of theory to give the gas-phase free energies and to confirm whether the structures are minima (no imaginary frequencies) or transition states (only one imaginary frequency). All transition-state structures were confirmed to connect the proposed reactants and products by intrinsic reaction coordinate (IRC) calculations.[43] The effect of solvent was examined by performing single-point self-consistent reaction-field (SCRF) calculations based on the conductor-like polarizable continuum model (C-PCM) for gas-phase optimized structures. Toluene ($\varepsilon=2.379$) was used as the solvent, corresponding to the experimental conditions, and the atomic radii used for the C-PCM calculations were specified by using the UFF keyword. Solvation free energies (ΔG_{Tol}) were calculated by adding the solvation energies to the computed gas-phase relative free energies (ΔG_{298}). Truhlar and Zhao have pointed out that M06 is a functional with good accuracy "across-the-board" for transition metals, main-group thermochemistry, medium-range correlation energy, and barrier heights.[40] The results in this study are consistent with this statement. We found both the M06 and the commonly used B3LYP functionals support the same mechanism of the $InCl_3$-catalyzed reaction, but the former method is more accurate for the AuCl-catalyzed reactions, as the results are consistent with the high-level MP2 calculations. The calculated energy profiles at the B3LYP/6-31G* (LANL2DZ) level are given in the Supporting Information.

Acknowledgements

This work is financially supported by the National Natural Science Foundation of China (grant no. 21002073 and 20872105), the Wenzhou Science & Technology Bureau (No. Y20100003), and the Wenzhou University (startup funding to Y.X.). All computations were done on the High Performance Computation Platform of Wenzhou University.

[1] For reviews, see: a) A. S. K. Hashmi, *Angew. Chem.* **2010**, *122*, 5360–5369; *Angew. Chem. Int. Ed.* **2010**, *49*, 5232–5241; b) A. Fürstner, *Chem. Soc. Rev.* **2009**, *38*, 3208–3221; c) S. M. Abu Sohel, R.-S. Liu, *Chem. Soc. Rev.* **2009**, *38*, 2269–2281; d) E. Soriano, J. Marco-Contelles, *Acc. Chem. Res.* **2009**, *42*, 1026–1036; e) D. J. Gorin, B. D. Sherry, F. D. Toste, *Chem. Rev.* **2008**, *108*, 3351–3378; f) N. T. Patil, Y. Yamamoto, *Chem. Rev.* **2008**, *108*, 3395–3442; g) R. A. Widenhoefer, *Chem. Eur. J.* **2008**, *14*, 5382–5391; h) E. Jiménez-Núñez, A. M. Echavarren, *Chem. Rev.* **2008**, *108*, 3326–3350; i) Z. Li, C. Brouwer, C. He, *Chem. Rev.* **2008**, *108*, 3239–3265; j) A. Arcadi, *Chem. Rev.* **2008**, *108*, 3266–3325; k) B. Crone, S. F. Kirsch, *Chem. Eur. J.* **2008**, *14*, 3514–3522; l) H. C. Shen, *Tetrahedron* **2008**, *64*, 3885–3903; m) H. C. Shen, *Tetrahedron* **2008**, *64*, 7847–7870; n) E. Jiménez-Núñez, A. M. Echavarren, *Chem. Commun.* **2007**, 333–346; o) D. J. Gorin, F. D. Toste, *Nature* **2007**, *446*, 395–403; p) A. S. K. Hashmi, *Chem. Rev.* **2007**, *107*, 3180–3211; q) L. Zhang, J. Sun, S. A. Kozmin, *Adv. Synth. Catal.* **2006**, *348*, 2271–2296; r) A. S. K. Hashmi, G. J. Hutchings, *Angew. Chem.* **2006**, *118*, 8064–8105; *Angew. Chem. Int. Ed.* **2006**, *45*, 7896–7936; s) S. Ma, S. Yu, Z. Gu, *Angew. Chem.* **2006**, *118*, 206–209; *Angew. Chem. Int. Ed.* **2006**, *45*, 200–203.

[2] For reviews, see: a) S. Kirsch, *Synthesis* **2008**, 3183–3204; b) A. Fürstner, P. W. Davies, *Angew. Chem.* **2007**, *119*, 3478–3519; *Angew. Chem. Int. Ed.* **2007**, *46*, 3410–3449; c) J. Marco-Contelles, E. Soriano, *Chem. Eur. J.* **2007**, *13*, 1350–1357; d) C. Bruneau, *Angew. Chem.* **2005**, *117*, 2380–2386; *Angew. Chem. Int. Ed.* **2005**, *44*, 2328–2334; e) G. C. Lloyd-Jones, *Org. Biomol. Chem.* **2003**, *1*, 215–236.

[3] For reviews, see: a) K. C. Majumdar, P. Debnath, B. Roy, *Heterocycles* **2009**, *78*, 2661–2728; b) S. I. Lee, N. Chatani, *Chem. Commun.* **2009**, 371–384; c) S. Ma, *Chem. Rev.* **2005**, *105*, 2829–2871; d) L. A. Goj, T. B. Gunnoe, *Curr. Org. Chem.* **2005**, *9*, 671–685; e) I. Nakamura, Y. Yamamoto, *Chem. Rev.* **2004**, *104*, 2127–2198; f) F. Alonso, I. P. Beletskaya, M. Yus, *Chem. Rev.* **2004**, *104*, 3079–3160; g) C. Aubert, O. Buisine, M. Malacria, *Chem. Rev.* **2002**, *102*, 813–834.

[4] For selected computational studies, see: a) D. Garayalde, E. Gómez-Bengoa, X. Huang, A. Goeke, C. Nevado, *J. Am. Chem. Soc.* **2010**, *132*, 4720–4730; b) P. H.-Y. Cheong, P. Morganelli, M. R. Luzung, K. N. Houk, F. D. Toste, *J. Am. Chem. Soc.* **2008**, *130*, 4517–4526; c) C. Nieto-Oberhuber, P. Pérez-Galán, E. Herrero-Gómez, T. Lauterbach, C. Rodríguez, S. López, C. Bour, A. Rosellón, D. J. Cárdenas, A. M. Echavarren, *J. Am. Chem. Soc.* **2008**, *130*, 269–279; d) C. Nieto-Oberhuber, S. López, M. P. Muñoz, D. J. Cárdenas, E. Buñuel, C. Nevado, A. M. Echavarren, *Angew. Chem.* **2005**, *117*, 6302–6304; *Angew. Chem. Int. Ed.* **2005**, *44*, 6146–6148; e) C. Nieto-Oberhuber, M. P. Muñoz, E. Buñuel, C. Nevado, D. J. Cárdenas, A. M. Echavar-

ren, *Angew. Chem.* **2004**, *116*, 2456–2460; *Angew. Chem. Int. Ed.* **2004**, *43*, 2402–2406.

[5] a) L.-P. Liu, G. B. Hammond, *Org. Lett.* **2010**, *12*, 4640–4643; b) L.-P. Liu, B. Xu, M. S. Mashuta, G. B. Hammond, *J. Am. Chem. Soc.* **2008**, *130*, 17642–17643; c) G. Seidel, C. W. Lehmann, A. Fürstner, *Angew. Chem.* **2010**, *122*, 8644–8648; *Angew. Chem. Int. Ed.* **2010**, *49*, 8466–8470.

[6] a) J. Sun, M. P. Conley, L. Zhang, S. A. Kozmin, *J. Am. Chem. Soc.* **2006**, *128*, 9705–9710; b) L. Zhang, S. A. Kozmin, *J. Am. Chem. Soc.* **2004**, *126*, 11806–11807; c) Y. Wang, B. Lu, L. Zhang, *Chem. Commun.* **2010**, *46*, 9179–9181; d) Y.-Q. Zhang, D.-Y. Zhu, Z.-W. Jiao, B.-S. Li, F.-M. Zhang, Y.-Q. Tu, Z. Bi, *Org. Lett.* **2011**, *13*, 3458–3461.

[7] For selected examples, see: a) C. Khin, A. S. K. Hashmi, F. Rominger, *Eur. J. Inorg. Chem.* **2010**, 1063–1069; b) Y. Xia, A. S. Dudnik, V. Gevorgyan, Y. Li, *J. Am. Chem. Soc.* **2008**, *130*, 6940–6941; c) A. S. Dudnik, Y. Xia, Y. Li, V. Gevorgyan, *J. Am. Chem. Soc.* **2010**, *132*, 7645–7655; d) R.-X. Zhu, D.-J. Zhang, J.-X. Guo, J.-L. Mu, C.-G. Duan, C.-B. Liu, *J. Phys. Chem. A* **2010**, *114*, 4689–4696; e) D. Zuccaccia, L. Belpassi, F. Tarantelli, A. Macchione, *J. Am. Chem. Soc.* **2009**, *131*, 3170–3171; f) J. Zhang, W. Shen, L. Li, M. Li, *Organometallics* **2009**, *28*, 3129–3139; g) A. S. Dudnik, A. W. Sromek, M. Rubina, J. T. Kim, A. V. Kel'in, V. Gevorgyan, *J. Am. Chem. Soc.* **2008**, *130*, 1440–1452; h) C. Ferrer, A. M. Echavarren, *Angew. Chem.* **2006**, *118*, 1123–1127; *Angew. Chem. Int. Ed.* **2006**, *45*, 1105–1109; i) W. Li, Y. Li, J. Zhang, *Chem. Eur. J.* **2010**, *16*, 6447–6450.

[8] For selected examples, see: a) M. E. Krafft, D. V. Vidhani, J. W. Cran, M. Manoharan, *Chem. Commun.* **2011**, *47*, 6707–6709; b) C. M. Krauter, A. S. K. Hashmi, M. Pernpointner, *ChemCatChem* **2010**, *2*, 1226–1230; c) G. Kovács, A. Lledós, G. Ujaque, *Organometallics* **2010**, *29*, 3252–3260; d) R. S. Paton, F. Maseras, *Org. Lett.* **2009**, *11*, 2237–2240; e) T. L. Sordo, D. Ardura, *Eur. J. Org. Chem.* **2008**, 3004–3013; f) X. Li, S. Ye, C. He, Z.-X. Yu, *Eur. J. Org. Chem.* **2008**, 4296–4303; g) F.-Q. Shi, X. Li, Y. Xia, L. Zhang, Z.-X. Yu, *J. Am. Chem. Soc.* **2007**, *129*, 15503–15512.

[9] For selected examples, see: a) H.-H. Liao, R.-S. Liu, *Chem. Commun.* **2011**, *47*, 1339–1341; b) P. W. Davies, N. Martin, *Org. Lett.* **2009**, *11*, 2293–2296; c) S. Bhunia, R.-S. Liu, *J. Am. Chem. Soc.* **2008**, *130*, 16488–16489; d) G. Kovács, G. Ujaque, A. Lledós, *J. Am. Chem. Soc.* **2008**, *130*, 853–864; e) G.-Y. Lin, C.-Y. Yang, R.-S. Liu, *J. Org. Chem.* **2007**, *72*, 6753–6757; f) G. L. Hamilton, E. J. Kang, M. Mba, F. D. Toste, *Science* **2007**, *317*, 496–499; g) J. J. Lian, P. C. Chen, Y. P. Lin, H. C. Ting, R.-S. Liu, *J. Am. Chem. Soc.* **2006**, *128*, 11372–11373; h) Z. Zhang, C. Liu, R. E. Kinder, X. Han, H. Qian, R. A. Widenhoefer, *J. Am. Chem. Soc.* **2006**, *128*, 9066–9073.

[10] For recent examples, see: a) G. Zhou, J. Zhang, *Chem. Commun.* **2010**, *46*, 6593–6595; b) T. Wang, J. Zhang, *Chem. Eur. J.* **2011**, *17*, 86–90; c) L. Cui, Y. Peng, L. Zhang, *J. Am. Chem. Soc.* **2009**, *131*, 8394–8395; d) G. Zhang, L. Zhang, *J. Am. Chem. Soc.* **2008**, *130*, 12598–12599; e) C. A. Witham, P. Mauleón, N. D. Shapiro, B. D. Sherry, F. D. Toste, *J. Am. Chem. Soc.* **2007**, *129*, 5838–5839; f) D. J. Gorin, P. Dubé, F. D. Toste, *J. Am. Chem. Soc.* **2006**, *128*, 14480–14481; , F. D. Toste, *J. Am. Chem. Soc.* **2006**, *128*, 14480–14481; g) M. R. Luzung, J. P. Markham, F. D. Toste, *J. Am. Chem. Soc.* **2004**, *126*, 10858–10859.

[11] a) Y. Xia, G. Huang, *J. Org. Chem.* **2010**, *75*, 7842–7854; b) M. Pernpointner, A. S. K. Hashmi, *J. Chem. Theory Comput.* **2009**, *5*, 2717–2725.

[12] For selected reviews and examples, see: a) C. Nevado, A. M. Echavarren, *Synthesis* **2005**, 167–182; b) M.-Z. Wang, C.-Y. Zhou, Z. Guo, E. L.-M. Wong, .M.-K. Wong, C.-M. Che, *Chem. Asian J.* **2011**, *6*, 812–824; c) T. Kitamura, *Eur. J. Org. Chem.* **2009**, 1111–1125; d) J. Storch, J. Čermák, J. Karban, I. Císařová, J. Sýkora, *J. Org. Chem.* **2010**, *75*, 3137–3140; e) J. Mo, P. H. Lee, *Org. Lett.* **2010**, *12*, 2570–2573; f) R. S. Menon, A. D. Findlay, A. C. Bissember, M. G. Banwell, *J. Org. Chem.* **2009**, *74*, 8901–8903; g) D. Weber, M. A. Tarselli, M. R. Gagné, *Angew. Chem.* **2009**, *121*, 5843–5846; *Angew. Chem. Int. Ed.* **2009**, *48*, 5733–5736; h) N. Chernyak, V. Gevorgyan, *J. Am. Chem. Soc.* **2008**, *130*, 5636–5637; i) M. A. Tarselli, M. R. Gagné, *J. Org. Chem.* **2008**, *73*, 2439–2441; j) C. Liu, R. A. Widenhoefer, *Org. Lett.* **2007**, *9*, 1935–1938; k) T. Watanabe, S. Oishi, N. Fujii, H. Ohno, *Org. Lett.* **2007**, *9*, 4821–4824; l) C. Nevado, A. M. Echavarren, *Chem. Eur. J.* **2005**, *11*, 3155–3164; m) J. A. Tunge, L. N. Foresee, *Organometallics* **2005**, *24*, 6440–6444; n) T. Yao, M. A. Campo, R. C. Larock, *Org. Lett.* **2004**, *6*, 2677–2680; o) S. J. Pastine, S. W. Youn, D. Sames, *Org. Lett.* **2003**, *5*, 1055–1058; p) C. Jia, D. Piao, T. Kitamura, Y. Fujiwara, *J. Org. Chem.* **2000**, *65*, 7516–7522; q) X. Han, R. A. Widenhoefer, *Org. Lett.* **2006**, *8*, 3801–3804; r) C. Liu, R. A. Widenhoefer, *J. Am. Chem. Soc.* **2004**, *126*, 10250–10251; s) C. Liu, X. Han, X. Wang, R. A. Widenhoefer, *J. Am. Chem. Soc.* **2004**, *126*, 3700–3701; t) Z. Shi, C. He, *J. Org. Chem.* **2004**, *69*, 3669–3671.

[13] a) V. Mamane, P. Hannen, A. Fürstner, *Chem. Eur. J.* **2004**, *10*, 4556–4575; b) A. Fürstner, V. Mamane, *Chem. Commun.* **2003**, 2112–2113; c) A. Fürstner, V. Mamane, *J. Org. Chem.* **2002**, *67*, 6264–6267.

[14] For recent examples of $GaCl_3$-catalyzed reactions of alkynes, see: a) H.-J. Li, R. Guillot, V. Gandon, *J. Org. Chem.* **2010**, *75*, 8435–8449; b) F. d. J. Cortez, R. Sarpong, *Org. Lett.* **2010**, *12*, 1428–1431; c) Y. Zhu, Y. Guo, D. Xie, *J. Phys. Chem. A* **2007**, *111*, 9387–9392; d) S. M. Kim, S. I. Lee, K. Kim, Y. K. Chung, *Org. Lett.* **2006**, *8*, 5425–5428; e) E. M. Simmons, R. Sarpong, *Org. Lett.* **2006**, *8*, 2883–2886; f) S. I. Lee, S. H. Sim, S. M. Kim, K. Kim, Y. K. Chung, *J. Org. Chem.* **2006**, *71*, 7120–7123; g) N. Chatani, H. Inoue, T. Kotsuma, S. Murai, *J. Am. Chem. Soc.* **2002**, *124*, 10294–10295; h) H. Inoue, N. Chatani, S. Murai, *J. Org. Chem.* **2002**, *67*, 1414–1417.

[15] For reviews, see: a) J. S. Yadav, A. Antony, J. George, B. V. S. Reddy, *Eur. J. Org. Chem.* **2010**, 591–605; b) J. Augé, N. Lubin-Germain, J. Uziel, *Synthesis* **2007**, 1739–1764; c) J. Podlech, T. C. Maier, *Synthesis* **2003**, 0633–0655; d) K. K. Chauhan, C. G. Frost, *J. Chem. Soc. Perkin Trans. 1* **2000**, 3015–3019.

[16] a) B. Montaignac, M. R. Vitale, V. Michelet, V. Ratovelomanana-Vidal, *Org. Lett.* **2010**, *12*, 2582–2585; b) T. Tsuchimoto, H. Matsubayashi, M. Kaneko, Y. Nagase, T. Miyamura, E. Shirakawa, *J. Am. Chem. Soc.* **2008**, *130*, 15823–15835; c) Y. Miyanohana, N. Chatani, *Org. Lett.* **2006**, *8*, 2155–2158.

[17] For recent applications of 1-haloalkynes in synthesis, see: a) A. Trofimov, N. Chernyak, V. Gevorgyan, *J. Am. Chem. Soc.* **2008**, *130*, 13538–13539; b) M. Yamagishi, K. Nishigai, T. Hata, H. Urabe, *Org. Lett.* **2011**, *13*, 4873–4875; c) Z. Chen, H. Jiang, A. Wang, S. Yang, *J. Org. Chem.* **2010**, *75*, 6700–6703.

[18] For reviews on transition-metal-triggered alkyne–vinylidene rearrangements, see: a) J. M. Lynam, *Chem. Eur. J.* **2010**, *16*, 8238–8247; b) B. M. Trost, A. McClory, *Chem. Asian J.* **2008**, *3*, 164–194; c) R.-S. Liu, *Synlett* **2008**, 801–812; d) C. Bruneau, P. H. Dixneuf, *Angew. Chem.* **2006**, *118*, 2232–2260; *Angew. Chem. Int. Ed.* **2006**, *45*, 2176–2203; e) J. A. Varela, C. Saá, *Chem. Eur. J.* **2006**, *12*, 6450–6456; f) Y. Wakatsuki, *J. Organomet. Chem.* **2004**, *689*, 4092–4109; g) F. E. McDonald, *Chem. Eur. J.* **1999**, *5*, 3103–3106; h) C. Bruneau, P. H. Dixneuf, *Acc. Chem. Res.* **1999**, *32*, 311–323; i) M. I. Bruce, *Chem. Rev.* **1991**, *91*, 197–257.

[19] The involvement of the Au–vinylidene intermediate in the gold-catalyzed cycloisomerization of propargylpyridines was ruled out by a recent computational and experimental study, see: Y. Xia, A. S. Dudnik, Y. Li, V. Gevorgyan, *Org. Lett.* **2010**, *12*, 5538–5541. During the publication process of this paper, the generation of Au-vinylidene from terminal alkynes was reported by Zhang et al., see: L. Ye, Y. Wang, D. H. Aue, L. Zhang, *J. Am. Chem. Soc.* **2012**, *134*, 31–34.

[20] a) For selected halogen migrations, see: J. Mátrai, A. Dransfeld, T. Veszprémi, M. T. Nguyen, *J. Org. Chem.* **2001**, *66*, 5671–5678; b) S. Bombek, R. Lenaršič, M. Kočevar, L. Saint-Jalmes, J.-R. Desmurs, S. Polanc, *Chem. Commun.* **2002**, 1494–1495; c) W. E. Billups, A. N. Kurtz, M. L. Farmer, *Tetrahedron* **1970**, *26*, 1095–1099; d) Y. M. Pustovit, A. N. Alekseenko, N. D. Volkov, M. Y. Fedorchuk, A. B. Rozhenko, *J. Fluorine Chem.* **2010**, *131*, 254–260.

[21] A. W. Sromek, M. Rubina, V. Gevorgyan, *J. Am. Chem. Soc.* **2005**, *127*, 10500–10501.
[22] a) E. Clot, *Eur. J. Inorg. Chem.* **2009**, 2319–2328; b) G. Lemière, V. Gandon, N. Agenet, J.-P. Goddard, A. de Kozak, C. Aubert, L. Fensterbank, M. Malacria, *Angew. Chem.* **2006**, *118*, 7758–7761; *Angew. Chem. Int. Ed.* **2006**, *45*, 7596–7599.
[23] E. Soriano, J. Marco-Contelles, *Organometallics* **2006**, *25*, 4542–4553.
[24] a) Z. J. Wang, D. Benitez, E. Tkatchouk, W. A. Goddard, F. D. Toste, *J. Am. Chem. Soc.* **2010**, *132*, 13064–13071; b) D. Benitez, E. Tkatchouk, A. Z. Gonzalez, W. A. Goddard, F. D. Toste, *Org. Lett.* **2009**, *11*, 4798–4801; c) D. Benitez, N. D. Shapiro, E. Tkatchouk, Y. Wang, W. A. Goddard, F. D. Toste, *Nat. Chem.* **2009**, *1*, 482–486.
[25] For recent examples of $PtCl_2$-catalyzed reactions, see: a) J. Li, C. Sun, S. Demerzhan, D. Lee, *J. Am. Chem. Soc.* **2011**, *133*, 12964–12967; b) C.-M. Ting, C.-D. Wang, R. Chaudhuri, R.-S. Liu, *Org. Lett.* **2011**, *13*, 1702–1705; c) H. Zheng, J. Zheng, B. Yu, Q. Chen, X. Wang, Y. He, Z. Yang, X. She, *J. Am. Chem. Soc.* **2010**, *132*, 1788–1789; d) S. Y. Kim, Y. Park, Y. K. Chung, *Angew. Chem.* **2010**, *122*, 425–428; *Angew. Chem. Int. Ed.* **2010**, *49*, 415–418; e) D. Vasu, A. Das, R.-S. Liu, *Chem. Commun.* **2010**, *46*, 4115–4117; f) S. Yang, Z. Li, X. Jian, C. He, *Angew. Chem.* **2009**, *121*, 4059–4061; *Angew. Chem. Int. Ed.* **2009**, *48*, 3999–4001.
[26] a) D. G. Truhlar, *J. Am. Chem. Soc.* **2008**, *130*, 16824–16827; b) Y. Zhao, D. G. Truhlar, *J. Chem. Theory Comput.* **2009**, *5*, 324–333.
[27] For recent examples, see: a) T.-A. Chen, T.-J. Lee, M.-Y. Lin, S. M. A. Sohel, E. W.-G. Diau, S.-F. Lush, R.-S. Liu, *Chem. Eur. J.* **2010**, *16*, 1826–1833; b) S. Ma, J. Zhang, *J. Am. Chem. Soc.* **2003**, *125*, 12386–12387; c) J. Chen, S. Ma, *Chem. Asian J.* **2010**, *5*, 2415–2421; d) S. Chuprakov, V, Gevorgyan, *Org. Lett.* **2007**, *9*, 4463–4466; e) Y. Zhang, F. Liu, J. Zhang, *Chem. Eur. J.* **2010**, *16*, 6146–6150; f) B. Alcaide, P. Almendros, T. M. del Campo, E. Soriano and J. L. Marco-Contelles, *Chem. Eur. J.* **2009**, *15*, 1901–1908; g) B. Alcaide, P. Almendros, T. M. del Campo, E. Soriano, J. L. Marco-Contelles, *Chem. Eur. J.* **2009**, *15*, 1909–1928; h) X. Jiang, X. Ma, Z. Zheng, S. Ma, *Chem. Eur. J.* **2008**, *14*, 8572–8578.
[28] a) T. Tsuchimoto, T. Maeda, E. Shirakawa, Y. Kawakami, *Chem. Commun.* **2000**, 1573–1574; b) D. S. Giera, C. Schneider, *Org. Lett.* **2010**, *12*, 4884–4887; c) B.-Y. Li, Z.-J. Li, X.-B. Meng, *Carbohydr. Res.* **2010**, *345*, 1708–1712; d) M. Dorbec, J.-C. Florent, C. Monneret, M.-N. Rager, C. Fosse, E. Bertounesque, *Eur. J. Org. Chem.* **2008**, 1723–1731; e) R. Hayashi, G. R. Cook, *Org. Lett.* **2007**, *9*, 1311–1314; f) J. S. Yadav, B. V. S. Reddy, B. Padmavani, *Synthesis* **2004**, 405–408.
[29] The results for $InCl_3$-catalyzed reactions from B3LYP/6–31G*-(LANL2DZ) calculations led to the same conclusion as the M06 calculations. Other possible intermolecular H-migrations are higher in energy. These results are given in the Supporting Information.
[30] For a recent example, see: a) G. O. Jones, P. Liu, K. N. Houk, S. L. Buchwald, *J. Am. Chem. Soc.* **2010**, *132*, 6205–6213; b) H.-Z. Yu, Y.-Y. Jiang, Y. Fu, L. Liu, *J. Am. Chem. Soc.* **2010**, *132*, 18078–18091.
[31] If the Br atom is replaced with an H atom, the structure will be nearly planar with H-C10-C1-Me, H-C10-C9-Au, and H-C10-C9-Cy dihedral angles being 2.58, −7.96, and 172.54°, respectively; see the Supporting Information for details.
[32] a) V. López-Carrillo, N. Huguet, A. Mosquera, A. M. Echavarren, *Chem. Eur. J.* **2011**, *17*, 10972–10978; b) A. M. Echavarren, *Nat. Chem.* **2009**, *1*, 431–433; c) A. Fürstner, L. Morency, *Angew. Chem.* **2008**, *120*, 5108–5111; *Angew. Chem. Int. Ed.* **2008**, *47*, 5030–5033; d) A. S. K. Hashmi, *Angew. Chem.* **2008**, *120*, 6856–6858; *Angew. Chem. Int. Ed.* **2008**, *47*, 6754–6756; e) P. Pérez-Galán, N. J. A. Martin, A. G. Campaña, D. J. Cárdenas, A. M. Echavarren, *Chem. Asian J.* **2011**, *6*, 482–486.
[33] a) P. A. Vadola, D. Sames, *J. Am. Chem. Soc.* **2009**, *131*, 16525–16528; b) M. Tobisu, H. Nakai, N. Chatani, *J. Org. Chem.* **2009**, *74*, 5471–5475; c) G. B. Bajracharya, N. K. Pahadi, I. D. Gridnev, Y. Yamamoto, *J. Org. Chem.* **2006**, *71*, 6204–6210.
[34] The lengths of Pt−C single bonds should be 2.08 and 1.98 Å for sp^3 and sp^2 carbon atoms, respectively, see: G. K. Anderson in *Comprehensive Organometallic Chemistry II, Vol. 9* (Eds: E. W. Abel, F. G. A. Stone, G. Wilkinson), Pergamon, New York, **1995**, and references therein.
[35] E. Soriano, J. Marco-Contelles, *J. Org. Chem.* **2007**, *72*, 1443–1448.
[36] N. M. Kostic, R. F. Fenske, *Organometallics* **1982**, *1*, 974–982.
[37] G. S. Hammond, *J. Am. Chem. Soc.* **1955**, *77*, 334–338.
[38] For selected recent examples, see: a) K.-G. Ji, X.-Z. Shu, J. Chen, S.-C. Zhao, Z.-J. Zheng, L. Lu, X.-Y. Liu, Y.-M. Liang, *Org. Lett.* **2008**, *10*, 3919–3922; b) X.-Z. Shu, X.-Y. Liu, K.-G. Ji, H.-Q. Xiao, Y.-M. Liang, *Chem. Eur. J.* **2008**, *14*, 5282–5289; c) A. S. Dudnik, N. Chernyak, V. Gevorgyan, *Aldrichimica Acta* **2010**, *43*, 37–46; d) R. Chaudhuri, A. Das, H.-Y. Liao, R.-S. Liu, *Chem. Commun.* **2010**, *46*, 4601–4603.
[39] Gaussian 09, Revision A.01, M. J. Frisch, G. W. Trucks, H. B. Schlegel, G. E. Scuseria, M. A. Robb, J. R. Cheeseman, G. Scalmani, V. Barone, B. Mennucci, G. A. Petersson, H. Nakatsuji, M. Caricato, X. Li, H. P. Hratchian, A. F. Izmaylov, J. Bloino, G. Zheng, J. L. Sonnenberg, M. Hada, M. Ehara, K. Toyota, R. Fukuda, J. Hasegawa, M. Ishida, T. Nakajima, Y. Honda, O. Kitao, H. Nakai, T. Vreven, J. A. Montgomery, Jr., J. E. Peralta, F. Ogliaro, M. Bearpark, J. J. Heyd, E. Brothers, K. N. Kudin, V. N. Staroverov, R. Kobayashi, J. Normand, K. Raghavachari, A. Rendell, J. C. Burant, S. S. Iyengar, J. Tomasi, M. Cossi, N. Rega, J. M. Millam, M. Klene, J. E. Knox, J. B. Cross, V. Bakken, C. Adamo, J. Jaramillo, R. Gomperts, R. E. Stratmann, O. Yazyev, A. J. Austin, R. Cammi, C. Pomelli, J. W. Ochterski, R. L. Martin, K. Morokuma, V. G. Zakrzewski, G. A. Voth, P. Salvador, J. J. Dannenberg, S. Dapprich, A. D. Daniels, Ö. Farkas, J. B. Foresman, J. V. Ortiz, J. Cioslowski, D. J. Fox, Gaussian, Inc., Wallingford CT, **2009**.
[40] a) Y. Zhao, D. G. Truhlar, *Theor. Chem. Acc.* **2008**, *120*, 215–241; b) Y. Zhao, D. G. Truhlar, *Acc. Chem. Res.* **2008**, *41*, 157–167.
[41] a) W. J. Hehre, R. Ditchfield, J. A. Pople, *J. Chem. Phys.* **1972**, *56*, 2257–2261; b) P. C. Hariharan, J. A. Pople, *Theor. Chim. Acta* **1973**, *28*, 213–222.
[42] a) P. J. Hay, W. R. Wadt, *J. Chem. Phys.* **1985**, *82*, 270–283; b) W. R. Wadt, P. J. Hay, *J. Chem. Phys.* **1985**, *82*, 284–298; c) P. J. Hay, W. R. Wadt, *J. Chem. Phys.* **1985**, *82*, 299–310.
[43] a) C. Gonzalez, H. B. Schlegel, *J. Chem. Phys.* **1989**, *90*, 2154–2161; b) C. Gonzalez, H. B. Schlegel, *J. Phys. Chem.* **1990**, *94*, 5523–5527.

Received: August 29, 2011
Revised: January 6, 2012
Published online: March 20, 2012

